HHS Public Access

Author manuscript

Mol Microbiol. Author manuscript; available in PMC 2021 May 14.

Published in final edited form as:

Mol Microbiol. 2021 April ; 115(4): 554–573. doi:10.1111/mmi.14623.

Staphylococcus aureus lacking a functional MntABC manganese import system have increased resistance to copper.

Hassan Al-Tameemi[1], **William N. Beavers**[2], **Javiera Norambuena**[1], **Eric P. Skaar**[2], **Jeffrey M. Boyd**[1,*]

[1]Department of Biochemistry and Microbiology, Rutgers, the State University of New Jersey, New Brunswick, NJ 08901

[2]Department of Pathology, Microbiology, and Immunology, Vanderbilt University Medical Center, Nashville, TN 37232

Summary

S. aureus USA300 isolates utilize the *copBL* and *copAZ* gene products to prevent Cu intoxication. We created and examined a Δ*copAZ* Δ*copBL* mutant strain (*cop*-). The *cop*- strain was sensitive to Cu and accumulated intracellular Cu. We screened a transposon (Tn) mutant library in the *cop*- background and isolated strains with Tn insertions in the *mntABC* operon that permitted growth in the presence of Cu. The mutations were in *mntA* and they were recessive. Under the growth conditions utilized, MntABC functioned in manganese (Mn) import. When cultured with Cu, strains containing a *mntA::Tn* accumulated less Cu than the parent strain. Mn(II) supplementation improved growth when *cop*- was cultured with Cu and this phenotype was dependent upon the presence of MntR, which is a repressor of *mntABC* transcription. A Δ*mntR* strain had an increased Cu load and decreased growth in the presence of Cu, which was abrogated by introduction of *mntA::Tn*. Over-expression of *mntABC* increased cellular Cu load and sensitivity to Cu. The presence of a *mntA::Tn* mutation protected iron-sulfur (FeS) enzymes from inactivation by Cu. The data presented are consistent with a model wherein defective MntABC results in decreased cellular Cu accumulation and protection to FeS enzymes from Cu poisoning.

Abbreviated Summary:

To combat antibiotic resistance, we need to develop new prevention and therapeutic approaches. Copper (Cu) has shown promise as an antimicrobial compound; however, questions remain about how Cu enters cells, kills microorganisms, and how microorganisms prevent intoxication by Cu. Here we present data showing that a dysfunctional MntABC Mn transporter results in decreased cellular Cu accumulation. We also demonstrate that cytosolic Cu accumulation inhibits *S. aureus* FeS enzymes.

[*]**Corresponding Author:** Jeffrey M. Boyd, Ph.D., Rutgers University, Department of Biochemistry and Microbiology, 76 Lipman Dr., New Brunswick NJ 08901, Phone: (848) 932-5604, FAX: (848) 932-8965, jeffboyd@SEBS.Rutgers.edu.

Author Contributions: (i) the conception or design of the study: JMB and HAT; (ii) the acquisition, analysis, or interpretation of the data: HAT, WNB, JN, EPS, and JMB; and (iii) writing of the manuscript: HAT and JMB.

Data Availability Statement:

The data that support the findings of this study are available from the corresponding author upon reasonable request.

Keywords

Staphylococcus aureus; manganese; copper; MntABC; iron-sulfur cluster

Introduction

Staphylococcus aureus continues to be a serious public health concern as *S. aureus* infections result in high morbidity and mortality rates (Turner *et al.*, 2019). Although historically known as a nosocomial pathogen, there has been an increase in community-acquired (CA) *S. aureus* cases among both immunocompetent and immunocompromised groups (Tenover *et al.*, 2006). These CA *S. aureus* strains often cause skin and soft tissue infections that can develop into invasive and systemic infections (Turner *et al.*, 2019). Treatment of *S. aureus* infections is complicated due to the ability of this pathogen to evolve and/or acquire resistance to antibiotics (Malachowa & DeLeo, 2010). To combat these problems, we need to develop new prevention and therapeutic approaches including the characterization of new promising antimicrobial targets.

Copper (Cu) is gaining popularity as an antimicrobial but killing or preventing growth of microorganisms using Cu is an age-old technology (Dollwet & Sorenson, 1985, Grass *et al.*, 2011). Copper is increasingly used as an intrinsic antibacterial and in metallic copper or copper-containing alloys on touch surfaces (Grass *et al.*, 2011). Mammals also use Cu to help clear infections by increasing Cu loads at sites of inflammation (Hodgkinson & Petris, 2012, Beveridge *et al.*, 1985). Cu accumulates within macrophage intracellular vesicles (Achard *et al.*, 2012) and ultimately in phagosomes (Wagner *et al.*, 2005). The addition of Cu to macrophages increases killing efficiency and genetic depletion of the Cu transporter ATP7A suppressed macrophage-dependent bacterial killing suggesting that macrophages that are defective in trafficking Cu to the phagolysome have a decreased ability to kill bacterial pathogens (White *et al.*, 2009). Bacterial pathogens, including *S. aureus*, that are defective in exporting Cu from the cytosol have decreased survival in macrophages and in other models of infection (Purves *et al.*, 2018, White *et al.*, 2009, Zapotoczna *et al.*, 2018, Ladomersky *et al.*, 2017).

Copper is an important micronutrient in some organisms (Andreini *et al.*, 2008) but, as alluded to above, cytosolic Cu overload results in intoxication (Purves *et al.*, 2018). Various mechanisms have been proposed to explain the toxic effects of Cu; however, the molecular mechanism(s) of Cu poisoning is not entirely clear, and it is likely multifaceted. In support of this, Cu intoxication involves perturbations of many stress and non-stress regulons resulting in multi-dimensional responses (Moore *et al.*, 2005, Baker *et al.*, 2010, Chillappagari *et al.*, 2010, Quintana *et al.*, 2017).

Metalloproteins often have an essential requirement for their cognate metal cofactor (Imlay, 2014). Solvent-accessible protein-associated metal ions can be displaced by oxidative stress or by alternate metals (Xu & Imlay, 2012, Gardner & Fridovich, 1991, Anjem & Imlay, 2012). Metalloproteins can also be mismetalated during maturation or oxidative stress (Waldron & Robinson, 2009, Gu & Imlay, 2013). Accumulation of Cu in the cytosol decreases the activities of iron-sulfur (FeS) enzymes (Macomber & Imlay, 2009, Djoko &

McEwan, 2013). Biochemical studies found that Cu can poison enzymes with solvent-exposed FeS clusters by disrupting the FeS cluster (Macomber & Imlay, 2009). Cu can also inhibit the assembly of FeS proteins by forming stable complexes with FeS cluster synthesis machineries and/or FeS protein maturation factors (Tan *et al.*, 2017, Chillappagari *et al.*, 2010, Tan *et al.*, 2014, Brancaccio *et al.*, 2017). It was recently shown that glyceraldehyde-3-phosphate dehydrogenase is also poisoned by Cu in *S. aureus* (Tarrant *et al.*, 2019).

Intoxication of *Streptococcus pneumoniae* by Cu was alleviated by the addition of manganese (Mn) to the growth medium (Johnson *et al.*, 2015). Accumulation of cytosolic Cu led to increased expression of proteins in the nucleotide synthesis pathway including the anaerobic ribonucleotide reductase system (NrdDG) suggesting that cells were starved for deoxynucleotide triphosphates (dNTPs). The aerobic ribonucleotide reductase system (NrdEF) is Mn-dependent (Martin & Imlay, 2011). A *S. pneumoniae* Δ*nrdD* mutant was more sensitive than the parent to Cu intoxication. These data led to the hypothesis that Cu inhibits aerobic dNTP synthesis by mismetalation of NrdF.

All *S. aureus* contain the *copAZ* operon (Sitthisak *et al.*, 2007). CopA is a transmembrane P1-type Cu(I) exporting ATPase (Arguello *et al.*, 2007) and CopZ is a cytosolic Cu(I)-binding chaperone that can deliver Cu(I) to CopA for export (Singleton *et al.*, 2009). We and others have recently shown that some *S. aureus* strains also contain the *copBL* operon to aid Cu detoxification (Rosario-Cruz *et al.*, 2019, Purves *et al.*, 2018). CopB is a P1-type Cu exporting ATPase and genetic evidence suggests that it has a degree of functional redundancy with CopA (Rosario-Cruz *et al.*, 2019). CopL is an external Cu binding lipoprotein that aids in preventing Cu from entering the cell (Rosario-Cruz *et al.*, 2019). Some strains also encode a multicopper oxidase (Mco) and a *S. aureus* Δ*mco* mutant was more sensitive to Cu than the parental strain (Zapotoczna *et al.*, 2018). *S. aureus* contain *csoR* which encodes for a transcriptional regulator of the *copBL* and *copAZ* operons (Grossoehme *et al.*, 2011, Purves *et al.*, 2018). Upon binding to Cu(I), holo-CsoR relieves repression of *copBL* and *copAZ* (Grossoehme *et al.*, 2011, Purves *et al.*, 2018).

During infection, the host restricts the bioavailability of metal ions including Mn (Becker & Skaar, 2014). To overcome Mn limitation, *S. aureus* employ two Mn uptake systems (Horsburgh *et al.*, 2002, Kehl-Fie *et al.*, 2013). The *mntABC* operon encodes for an ATPase to provide energy for uptake (MntA), a permease (MntB), and an extracellular Mn binding lipoprotein (MntC) (Gribenko *et al.*, 2013). The *mntH* gene encodes a Mn permease of the NRAMP family (Que & Helmann, 2000, Horsburgh *et al.*, 2002). Cytosolic Mn is sensed by the transcriptional regulator MntR. When associated with Mn, holo-MntR represses *mntABC* transcription by binding to the promoter of *mntA* (Horsburgh *et al.*, 2002, Glasfeld *et al.*, 2003, Handke *et al.*, 2013).

Given the inherent differences between bacterial species, the cellular targets of Cu intoxication are likely not universal, and the goal of this study was to investigate how Cu toxifies *S. aureus*. To this end, we constructed a strain that is defective in copper detoxification (*cop*- strain). This strain was sensitive to Cu and it accumulated Cu. We screened for *cop*- strains that had increased tolerance to Cu. Strains containing transposon (Tn) insertions in *mntA* were protected against Cu intoxication. The data presented herein

are consistent with the hypothesis that *S. aureus* with defective MntABC permease have decreased Cu uptake which protects FeS enzymes from Cu poisoning. These findings highlight the challenges that organisms face when trying to acquire an essential micronutrient and help to explain why having redundant tightly regulated systems such as MntH and MntABC to uptake metals is beneficial.

Results

A *S. aureus* Δ*copBL* Δ*copAZ* strain accumulates intracellular Cu.

We created a Δ*copAZ* Δ*copBL* strain in the USA300_LAC background. We compared the growth of the Δ*copAZ* Δ*copBL* strain to that of the wild type (WT), Δ*copAZ*, and Δ*copBL* strains. When compared to the growth of the WT, the Δ*copBL* strain was more sensitive to growth on solid medium in the presence of Cu whereas the Δ*copAZ* displayed little to no Cu sensitivity phenotype (Figure 1A). The Δ*copAZ* Δ*copBL* double mutant was more sensitive to Cu than the Δ*copAZ* and Δ*copBL* strains. We henceforth refer to the Δ*copAZ* Δ*copBL* strain as *cop*-.

We hypothesized that the *copAZ* and *copBL* are the primary genetically encoded elements in LAC specifically utilized for Cu ion homeostasis. CsoR is a transcriptional repressor that relieves repression of genes within its regulon when it is bound to Cu (Ma *et al.*, 2009, Grossoehme *et al.*, 2011). We created a *cop*- Δ*csoR* strain and found that this strain phenocopied the *cop*- strain (Figure 1B). Although not conclusive, these data are consistent with the hypothesis that *copAZ* and *copBL* are the primary Cu detoxification genes transcriptionally controlled by CsoR in USA300_LAC.

We tested the hypothesis that the *cop*- strain accumulated intracellular Cu. We used inductively coupled plasma mass spectrometry (ICP-MS) to monitor total Cu load in the WT and *cop*- strains after culturing in the presence and absence of 10 μM Cu(II). After co-culture with Cu in tryptic soy broth (TSB), both strains accumulated Cu; however, the *cop*- strain accumulated much more Cu (Figure 1C). There was not a noticeable difference in Cu load between the WT and *cop*- strains after culture in TSB. The overall cellular Mn load of the cultures was not significantly affected. Co-culture with 10 μM Cu(II) did not result in an appreciable decrease in cell pellet weight (Figure S1A) or significant growth defect (Figure S1B) in the *cop*- strain.

Mutational analyses provide insight into copper homeostasis.

We built a transposon (Tn) library in the *cop*- strain. We plated cells from the Tn mutant library and ten strains were isolated that grew with 2.5 mM Cu(II). After reconstruction and phenotypic verification, we mapped the transposon mutations to three locations. Two strains had mutations in *mntA* of the *mntABC* operon. One strain had a mutation in *apt*, which encodes a predicted adenine phosphoribosyltransferase. Seven strains had mutations in *ispA*, which encodes a geranylgeranyl diphosphate synthase II. All mutants provided a similar growth advantage when cultured on Cu containing solid medium (Figure 2A). For the purposes of this study we focused efforts on determining why the *mntA::Tn* strains permitted growth in the presence of Cu(II). The *mntA::Tn* insertions were located at the

TA/AT sites located at +84 (*mntA1::Tn*) and +91 (*mntA2::Tn*). When cultured in the presence of Cu(II) the *mntA::Tn* mutants phenocopied one another. For simplicity, only the *mntA1::Tn* mutation was further investigated. The *mntA1::Tn* allele also improved the growth of the *cop*- strain in liquid TSB (Figure 2B).

The *mntA1::Tn* mutations are recessive.

The *cop*- *mntA1::Tn* displayed increased growth when compared to the *cop*- strain when cultured in the presence of Cu(II) on solid or liquid TSB medium (Figure 2), as well as in liquid defined medium (Figure 3A). The finding that suppression also occurred in defined medium allows us to expand phenotypic analyses. When we returned the *mntABC* genes at a secondary chromosomal location, the resulting *cop*- *mntA1::Tn* pLL39_*mntABC* strain grew similar to the *cop*- pLL39 (empty vector) strain. These data suggested that the *mntA1::Tn* mutations were recessive.

To further explore this idea, we created a *cop*- Δ*mntA::tetR* strain. The *mntA::tetR* mutation provided a growth advantage in medium containing Cu(II), but it did not provide as robust of a growth advantage as the *mntA1::Tn* mutation (Figure 3B). We hypothesized that this was due to the *mntA1::Tn* mutation having polar effects on downstream operon components. We compared the growth of the *cop*- Δ*mntA::tetR, cop*- Δ*mntB::tetR,* and *cop*- *mntC::Tn* strains in the presence and absence of Cu(II). Whereas all three mutants showed better growth than the *cop*- strain when cultured with Cu(II), the Δ*mntB::tetR* and Δ*mntC::Tn* mutants provided better growth than the Δ*mntA::tetR* mutation (Figure 3C). The growth of the Δ*mntB::Tn* strain phenocopied that of the *mntA::Tn* strain (Figure 4D). None of the *mnt* mutant strains had a growth defect or growth advantage in the absence of Cu under the growth conditions utilized (data not shown).

We tested the hypothesis that the *mntABC* gene products work in conjunction with one another to provide enhanced growth in the presence of Cu(II). We created *cop*- Δ*mntAB::tetR*, and *cop*- Δ*mntABC::tetR* strains and compared them to the growth of the *cop*- Δ*mntB::tetR* strain. The strains containing the Δ*mntB::tetR*, Δ*mntAB::tetR*, and Δ*mntABC::tetR* mutations phenocopied one another and all three had enhanced growth in the presence of Cu(II) when compared to the *cop*- strain (Figure 3D). Taken together, these data suggested that the *mntA1::Tn* mutation had polar effects on expression of downstream operon components and that mutations in any of the *mntABC* genes was sufficient to suppress the Cu(II) sensitivity phenotype of the *cop*- strain.

The small RNA RsaC does not modulate the Cu(II) sensitivity of the *cop*- strain.

The *rsaC* gene encodes for a small RNA that is located downstream of *mntC* and is co-transcribed with *mntABC* in response to Mn starvation (Lalaouna *et al.*, 2019). We examined whether *rsaC* has a role in 1) in the Cu(II) sensitivity phenotype of the *cop*- strain, and 2) in the growth advantage phenotype afforded by the *mntA1::Tn* insertion mutation. The *cop*- Δ*rsaC::tetM* strain phenocopied the *cop*- strain on TSB medium supplemented with Cu(II) (Figure S2). The *cop*- *mntA1::Tn* and *cop*- *mntA1::Tn* Δ*rsaC::tetM* strains also phenocopied one another and both strains grew better than the *cop*- strain in the presence of Cu(II).

To further explore the role of *rsaC* in Cu(II) homeostasis, we created vectors that expressed *rsaC* either in the sense or antisense orientation. The plasmid encoded *rsaC* variants were under the transcriptional control of an anhydrotetracycline inducible promoter. The *cop*- strain containing the empty vector (pML100) or the vectors expressing *rsaC* cloned in the sense (pML100_*rsaC*) or antisense (pML100_*rsaC*-antisense) direction behaved identical when plated on TSB medium with or without Cu(II) (Figure S3). As a control for *rsaC* expression, we also plated the same strains on TSB medium supplemented with the reactive oxygen species generating molecule methyl viologen. Strains that overproduce *rsaC* are sensitive to methyl viologen as a result of decreased superoxide dismutase (*sodA*) expression (Lalaouna *et al.*, 2019). The *cop*- strain containing the pML100_*rsaC* had decreased growth in the presence of inducer and methyl viologen when compared to the *cop*- strain containing pML100 or pML100_*rsaC*-antisense. The results further suggest that RsaC does not impact Cu(II) ion homeostasis in the *cop*- strain under the conditions examined.

The *mntA1::Tn* mutation results in decreased Cu accumulation

We tested the hypothesis that the *mntA1::Tn* mutation provides enhanced growth in the presence of Cu(II) by decreasing cellular Cu accumulation. Cultures were grown for eight hours before 0, 1, 5, or 10 μM Cu(II) was added. Cultures were incubated for an additional 15, 30, or 60 minutes before cells were harvested. Cells were washed to remove any adventitiously bound metal and cellular Cu and Mn were quantified using ICP-MS. Cu accumulated in both strains and it accumulated as a function of both time and the concentration of Cu(II) added. When compared with *cop*- strain, the *cop*- *mntA1::Tn* mutant accumulated less copper across all Cu concentrations of Cu utilized and all sampling times (Figure 4). Co-incubation with Cu(II) had little effect on the cellular Mn content. The *cop*- *mntA1* strain had slightly less Mn than the *cop*- strain at a few of the time points examined.

mntABC function in Mn homeostasis and are repressed by MntR in a manganese-dependent manner under the growth conditions utilized.

MntR was reported to act as a negative and positive regulator of *mntABC* and *mntH* in *S. aureus*, respectively (Horsburgh *et al.*, 2002). An alternate study found that *mntH* transcription was not altered as a variable of Mn concentration (Kehl-Fie *et al.*, 2013). We quantified *mntABC* and *mntH* transcripts in the *cop*- and *cop*- *mntR::tetR* strains after culturing in the presence and absence of 10 μM Mn(II). The transcription of *mntABC* was repressed in the presence of Mn(II) and this repression was dependent upon supplementing the growth medium with Mn(II) and the presence of MntR (Figure 5A). Under the growth conditions utilized, neither culturing with Mn(II), or the presence of MntR, had an effect on *mntH* transcription.

Treating TSB with Chelex resin decreases the concentrations of divalent metals. We cultured the *cop*- strain in TSB, TSB with 10 μM Mn(II), Chelex treated TSB, or Chelex treated TSB supplemented with 10 μM Mn(II) before quantifying *mntABC* transcripts. The transcription of *mntABC* was repressed when cells were cultured in TSB medium with Mn(II) when compared to cells cultured in TSB (Figure 5B). These data suggested that our laboratory TSB medium is not replete with Mn. Culturing in Chelex treated medium further increased transcription of *mntABC*. The addition of 10 μM Mn(II) to the Chelex treated medium

returned *mntABC* transcription to levels noted in the cells grown in TSB medium containing 10 μM Mn(II). These data suggested that we could further remove Mn from the TSB medium by treatment with Chelex.

We sought to verify a role for MntABC in Mn homeostasis in the growth conditions utilized herein. We cultured the *cop-* and *cop- mntA1::Tn* strains in Chelex-treated TSB before harvesting cells and determining Mn load using ICP-MS (Figure 5C). The *cop- mntA1::Tn* mutant had a lower Mn load than the *cop-* strain confirming a role for MntABC in Mn homeostasis under the growth conditions utilized.

Derepression of *mntABC* transcription results in increased Cu accumulation and toxicity.

We examined the effect of MntR-dependent regulation of *mntABC* on cellular Cu loads. The *cop-*, *cop- mntA1::Tn*, *cop- mntR::tetR*, and *cop- mntA1::Tn mntR::tetR* strains were cultured in Chelex-treated TSB before dosing the cells with and without 5 μM Cu(II). The cells were incubated for an additional 60 minutes before harvesting, washing away adventitiously associated metal, and quantifying cellular Cu and Mn pools. The *cop- mntA1::Tn* strain accumulated less Cu than the *cop-* strain (Figure 6A). The *cop- mntR::tetR* strain accumulated more Cu than the *cop-* strain; however, this Cu accumulation was dependent upon a functional MntABC. The *cop- mntA1::Tn mntR::tetR* strain had a Cu load that phenocopied that of the *cop- mntA1::Tn* strain. In general, the strains had similar Mn pools. The addition of Cu(II) did not have a significant effect on the Mn concentration associated with the *cop-* strain. The strains containing *mntA1::Tn* mutation had decreased Mn pools when compared to the *cop-* parent strain.

We tested the hypothesis that derepression of *mntABC* transcription would increase Cu sensitivity. The *cop-*, *cop- mntA1::Tn*, *cop- mntR::tetR*, and *cop- mntA1::Tn mntR::tetR* strains were spot-plated on solid TSB containing 1.75 or 2 mM Cu(II). The *cop- mntR::tetR* strain was more sensitive to Cu(II) than the *cop-* strain suggesting that removal of MntR-dependent repression of *mntABC* transcription increased sensitivity to Cu(II) (Figure 6B). The *cop- mntA1::Tn mntR::tetR* strain phenocopied the *cop- mntA1::Tn* strain.

The findings that MntR modulates Cu accumulation and homeostasis via MntABC and that our TSB medium is not replete with Mn led us to hypothesize that we could decrease sensitivity to Cu(II) by supplementing the growth medium with Mn(II). We examined the growth of *cop-*, *cop- mntA1::Tn*, *cop- mntR::tetR*, and *cop- mntA1::Tn mntR::tetR* strains with 1.75 or 2 mM Cu(II) in the presence and absence of 5 μM Mn(II). The presence of Mn(II) improved the growth of the *cop-* strain when cultured with Cu, but not the growth of the *cop- mntR* mutant (Figure 6B). The presence of Mn(II) did not alter the Cu(II) sensitivities of the *cop- mntA1::Tn* and *cop- mntA1::Tn mntR::tetR* strains.

Increased *mntABC* expression results in Cu sensitivity and Cu accumulation.

We tested the hypothesis that increased *mntABC* expression results in increased Cu(II) sensitivity and Cu accumulation. We placed *mntABC* under the transcriptional control of a xylose inducible promoter. When cultured in the presence of Cu(II), the *cop-* strain containing the plasmid pEPSA5_*mntABC* had decreased growth when compared to the *cop-*

strain containing the pEPSA5 (empty vector) (Figure 7A). The WT strain with pEPSA5_*mntABC* behaved like the WT strain containing pEPSA5.

We compared the total Cu loads of the *cop*- strain containing either pEPSA5_*mntABC* or pEPSA5. The *cop*- strain containing pEPSA5_*mntABC* had an increased Cu load compared to the *cop*- strain containing pEPSA5 (Figure 7B). These data are consistent with the hypotheses that overproduction of MntABC in the *cop*- strain results in increased Cu accumulation and that the WT strain, which contained *copAZ* and *copBL*, was able to detoxify Cu even when MntABC was over produced.

The lack of a functional MntABC protects FeS enzymes from Cu poisoning.

Recent work by Johnson *et al*. reported that the *Streptococcus pneumonia* aerobic Mn-dependent ribonucleotide reductase (NrdEF) is poisoned by Cu (Johnson *et al*., 2015). *S. aureus* utilizes the NrdEF and NrdDG ribonucleotide reductases primarily during aerobic and anaerobic growth, respectively (Cotruvo & Stubbe, 2012, Rabinovitch *et al*., 2010). We tested the hypothesis that the activity of essential NrdEF is decreased by intracellular Cu accumulation. The *cop*- and *cop*- *nrdD::Tn* strains were spot plated on solid medium with and without Cu and/or the ribonucleotide reductase inhibitor hydroxyurea. Hydroxyurea and Cu(II) individually inhibited the growth of the strain aerobically, but no difference was noted between the *cop*- and *cop*- *nrdD::Tn* strains (Figure S4). However, these compounds showed great synergy in inhibiting growth when provided simultaneously. The addition of Mn did not significantly affect growth in the presence of Cu or hydroxyurea. The *cop*- *nrdG::Tn* strain phenocopied the *cop*- *nrdD::Tn* strain (data not shown).

During anaerobic growth the *cop*- *nrdD::Tn* strain had smaller colony size phenotype and it was more sensitive to hydroxyurea than the *cop*- strain (Figure S4). Both strains had slow growth phenotype in the presence of Cu(II) and there was not a significant decrease in growth of the *cop*- *nrdD::Tn* strain with Cu(II) (Figure S5). There was not a synergistic effect of hydroxyurea and Cu. Taken together, these data suggest that NrdEF is not a primary target of Cu toxicity in *S. aureus*.

Intracellular Cu accumulation can directly and indirectly decrease the activities of enzymes that require solvent-exposed clusters (Macomber & Imlay, 2009, Tan *et al*., 2014). *S. aureus* utilizes the SufCDSUB machinery to synthesize iron–sulfur (FeS) clusters from monoatomic Fe^{2+}, S^0, and electrons (Roberts *et al*., 2017). We previously characterized a strain that contains a Tn insertion between the *sufC* and *sufD* genes (*sufD**) of the *sufCDSUB* operon. The *sufD** mutation results in decreased transcription of *suf* genes resulting in a decreased capacity to maturate FeS proteins (Roberts *et al*., 2017). When compared to the *cop*- strain, the *cop*- *sufD** strain had a greatly decreased growth when cultured with Cu(II) (Figure 8A). The presence of the *mntB::tetR* allele rescued the growth of the *cop*- *sufD** strain in the presence of Cu(II) (Figure 8B).

Previous work found that Cu inhibits Leu and Ile synthesis by inactivation of the FeS cluster-dependent dehydratases necessary to synthesize the amino acids (Macomber & Imlay, 2009). We also noted that the addition of 5 μM Cu(II) to defined medium lacking Leu and Ile inhibited the growth of the *cop*- strain (Figure 8C). The *cop*- strain was capable of

growth in defined medium containing 5 μM Cu(II) when it was supplemented with Leu and Ile (data not shown). The *cop- mntA1::Tn* strain was able to grow in defined medium containing 5 μM Cu(II) medium lacking Leu and Ile. These data suggested that the presence of the *mntA1::Tn* mutation protects FeS cluster containing dehydratases from inactivation in the presence of Cu.

We examined the effect of Cu(II) on aconitase (AcnA) activity, which is an FeS cluster-dependent dehydratase (Beinert *et al.*, 1996). For these experiments, we used a strain that contained a null *acnA* allele, and a secondary plasmid encoded *acnA* allele that was under the transcriptional control of a xylose inducible promoter (p*acnA*). This decreased the possibility that Cu was modulating *acnA* transcription. Growth in the presence of Cu(II) resulted in a concentration-dependent decrease in AcnA activity in the *cop- acnA::tetR* strain containing p*acnA*. AcnA activity was nearly undetectable after culture with 20 μM Cu(II) (Figure 8D). We next examined the effect of introducing the *mntA1::Tn* mutation on *in vivo* AcnA activity. The *cop- acnA::tetR mntA1::Tn* strain containing p*acnA* had decreased AcnA activity when cultured in the presence of Cu(II), but the decrease in activity was substantially less than that noted for the *cop- acnA::tetR* strain (Figure 8D).

We sought to determine if the *S. aureus* AcnA was poisoned by Cu *in vitro*. Cell lysates from the *cop-* strain were created anaerobically and then combined with Cu(II) before monitoring AcnA activity. The presence of Cu(II) decreased AcnA activity in a concentration dependent manner (Figure 8E). Ascorbate can reduce Cu(II) to Cu(I) which has a higher affinity for sulfur atoms and is a more avid disrupter of FeS clusters (Macomber & Imlay, 2009). We repeated the *in vitro* AcnA assays, but this time, when we co-incubated the lysates with Cu(II) we included 100 μM ascorbate in one-half of the samples. The inclusion of ascorbate did not enhance Cu-dependent poisoning of AcnA *in vitro* (Figure S6).

Discussion

The goal of this study was to investigate how Cu toxifies *S. aureus*. To this end, we created and examined a *S. aureus* strains lacking the CopAZ and CopBL Cu detoxification factors. As previously reported, the Δ*copBL* and Δ*copAZ* mutants had intermediate sensitivities to growth in the presence of Cu(II) whereas the phenotypes of the Δ*copBL* and Δ*copAZ* deletions displayed genetic synergy. The *cop-* (Δ*copBL* Δ*copAZ*) strain also had a high Cu load after dosing with Cu(II). CsoR represses Cu detoxification systems and a *cop-* Δ*csoR* strain had the same sensitivity to Cu(II) as the *cop-* strain. Although not conclusive, these data are consistent with the hypothesis that *copAZ* and *copBL* are the primary Cu detoxification genes in USA300_LAC that are under CsoR transcriptional control.

The data presented herein, in conjunction with our previous work, as well as work from others, has resulted in the following working model for Cu homeostasis in *S. aureus* (Figure 9). Under Mn deplete conditions, *mntABC* is expressed and Cu(II) enters *S. aureus* cells by a MntABC-dependent mechanism. Once inside, cellular reductants reduce Cu(II) to Cu(I) (Scarpa *et al.*, 1996, Rigo *et al.*, 2004, Ngamchuea *et al.*, 2016). The Cu(I) can associate with the CsoR transcriptional repressor resulting in derepression of the *copAZ* and *copBL*

operons (Grossoehme *et al.*, 2011, Rosario-Cruz *et al.*, 2019). CopA and CopB function as Cu(I) export systems (Grossoehme *et al.*, 2011, Purves *et al.*, 2018). CopZ acts as an intracellular Cu(I) binding protein that buffers the cytosol from Cu toxicity (Banci *et al.*, 2001). Holo-CopZ traffics Cu(I) to CopA for export (Singleton *et al.*, 2009). After export by CopA or CopB, or before Cu enters the cell, CopL binds to Cu(I) and prevents it from (re)entering (Rosario-Cruz *et al.*, 2019). Defective Cu removal results in poisoning of FeS cluster-dependent enzymes.

The *S. pneumoniae* genome encodes for the MntABC and MntR homologues PsaBCA and PsaR (Dintilhac *et al.*, 1997, McAllister *et al.*, 2004, Johnston *et al.*, 2006, Lisher *et al.*, 2013). PsaB is an ATPase and PsaA is a Mn-specific permease (Claverys, 2001). PsaA is a high-affinity is Mn(II) substrate-binding protein (SBP) that can also bind Zn(II) (Li *et al.*, 2014, McDevitt *et al.*, 2011). PsaA binding to Zn(II) can preclude Mn binding and PsaA association with Mn is thought to be necessary PsaBA-mediated Mn(II) import (Counago *et al.*, 2014). Therefore, Zn(II) association with PsaA can result in decreased Mn(II) influx (McDevitt *et al.*, 2011). Consistent with this, co-culturing *S. pneumoniae* with high levels of Zn(II) results in growth phenotypes that mimic that of a Δ*psaA* mutant. Thermostability and metal binding studies were used to show that PsaA can also associate with Cu(II) (Counago *et al.*, 2014). When co-cultured with Cu(II), the wild-type and Δ*psaA* strains had similar Cu accumulation suggesting that PsaBA does not import Cu in *S. pneumoniae*; however, it should be noted that these strains possessed the CopA Cu(I) exporter and the CupA Cu(I) chaperone possibly masking potential effects that the Δ*psaA* mutation had on cellular Cu accumulation (Counago *et al.*, 2014, Shafeeq *et al.*, 2011). The addition of Cu(II) to the growth medium did not significantly impact the concentration of Mn associated with the *S. aureus cop*- strain under the growth conditions utilized in our studies suggesting the Cu intoxication is not occurring by interfering with Mn uptake.

The *mntAB* gene products work in conjunction as an ABC transporter (Dintilhac *et al.*, 1997). Results herein show that the Δ*mntA::tetR* and Δ*mntB::tetR* mutants both suppressed the Cu sensitivity phenotype of the *cop*- strain; however, unexpectedly, the Δ*mntA::tetR* mutation did not suppress to the same extent as the Δ*mntB::tetR* or *mntA1::Tn* mutations. The genetic analyses presented show that the effects of the individual mutations were not additive suggesting that MntABC do work in conjunction with one another. Similar to the results presented herein, Novick *et al.* reported that strains with plasmid insertion mutations in *psaA*, *psaB*, or *psaC* resulted in strains with slightly different transformation efficiencies and adherence properties (Novak *et al.*, 1998). McAllister *et al.* created and analyzed a library of *psa* clean deletion mutants and reported that the individual *psa* mutants did not phenocopy one another (McAllister *et al.*, 2004). Lim *et al.* found that *Neisseria gonorrhoeae mntAB* and *mntC* mutants have different phenotypes with the *mntAB* mutant having a more severe growth defect and a small colony phenotype (Lim *et al.*, 2008). The authors hypothesized that in the absence of MntC, the permease still functions, but it has a lower affinity for the metals of interest. In this case, the authors hypothesized that MntABC transported both Zn and Mn. TcyABC is an ABC transporter for cystine in *Streptococcus mutans*. Kim et al. reported differential growth phenotypes of *tcyA*, *tycB,* and *tycC* mutant strains (Kim *et al.*, 2012). The *tcyABC* and *tcyC* mutants did not grow in low cysteine containing medium whereas the *tcyA* and *tcyB* mutants were capable of growth abet with a

slow growth phenotype. TcyA, TcyB, and TcyC are predicted to be an SBP, a permease, and an ATPase, respectively.

RsaC is a sRNA that is co-transcribed with *mntABC* in *S. aureus* (Lalaouna *et al.*, 2019). In the FPR3757 genome, the +1 of the *rsaC* coding region resides 113 base-pairs downstream of *mntC*. RsaC interacts with a number of mRNAs that function in ROS/RNS metabolism including *sodA* which encodes for a Mn-dependent superoxide dismutase. Five results are presented herein that suggest that *rsaC* is not involved in the increased Cu(II) ion resistance phenotype of the *cop- mntA1::Tn* strain under the growth conditions we utilized. First, we returned the *mntABC* genes in trans to the *cop- mntA1::Tn* mutant and found that they could complement the Cu sensitivity phenotype. Both the pLL39_*mntABC* and pEPSA5_*mntABC* vectors that we utilized lack the *rsaC* ORF and both plasmids work for genetic complementation of the Cu sensitivity phenotype of the *mntA::Tn* strain. Second, a *cop-* Δ*rsaC::tet* mutant strain displayed the same sensitivity to Cu(II) as the *cop-* strain. Third, the Δ*rsaC::tet* mutation did not alter the ability of the *mntA1::Tn* mutation to suppress the Cu(II) sensitivity phenotype of the *cop-* strain. Fourth, overproduction of *rsaC* did not alter the sensitivity of the *cop-* strain to Cu(II). Fifth, over-expression of *mntABC* using either pEPSA5_*mntABC* or a Δ*mntR* strain results in increased sensitivity to Cu and increased cellular Cu accumulation. Introduction of the *mntA1::Tn* allele nullified the effects of the Δ*mntR* mutation. Taken together, these findings are consistent with the hypothesis that the disruption of something within *mntABC* by the *mntA1::Tn* insertion improves growth in the presence of Cu(II) and this phenotype is independent of *rsaC* expression.

Compared to other transition metals, Cu uptake pathways are the least understood in bacterial pathogens and questions remain about how Cu enters cells (Begg, 2019). Dedicated Cu uptake systems have been described in *Rhodobacter capsulatus* and *Synechocystis* which require increased Cu loads for specific metabolic processes (Ekici *et al.*, 2012, Tottey *et al.*, 2001). A dedicated Cu import system has not been described for *S. aureus*.

A number of metals including lead (Pb), silver (Ag), cadmium (Cd) and mercury (Hg) have no described biological roles and are potent poisons of intracellular enzymes (Xu & Imlay, 2012, Jaroslawiecka & Piotrowska-Seget, 2014). For the most part, dedicated import systems for these metals do not exist. Positively charged metal ions have a difficult time passing through hydrophobic membranes, which has led to the hypothesis that these metals enter cells through import systems that function primarily to import alternate compounds that are required for proper functioning of the cell (Tynecka *et al.*, 1981, Laddaga & Silver, 1985). This is paradoxical because these transporters are expressed to allow entry of essential nutrients while maintaining an electrochemical gradient and preventing the entry of toxic compounds. Cellular systems have evolved to transform and/or efflux these toxic metals thereby decreasing cytosolic concentrations and maintaining homeostasis (Borremans *et al.*, 2001, Gupta *et al.*, 1999, Gaballa & Helmann, 2003, Norambuena *et al.*, 2017).

Metals such as Zn, Fe, Mn, and Cu, often have cellular roles, but cytosolic overload can be toxic (Chandrangsu & Helmann, 2016, Macomber & Imlay, 2009, Huang *et al.*, 2017, Guan *et al.*, 2015). The mechanisms of Mn, Zn, Fe acquisition have been thoroughly examined (reviewed here (Palmer & Skaar, 2016)). Nearly all described ABC transporters only

transport in one direction (Wilkens, 2015). In support of this, recent work has found that some bacteria utilize Mn, Zn, and Fe efflux systems to prevent cytosolic accumulation (Guan *et al.*, 2015, Huang *et al.*, 2017, Gaballa & Helmann, 2003, Chandrangsu *et al.*, 2017).

Many studies suggest that metal import is a promiscuous process, but few studies have identified and conclusively shown that metal uptake systems inadvertently uptake alternate metals. In *S. aureus*, Cd(II) uptake by membrane vesicles was decreased upon the addition of CCCP, valinomycin, or Mn(II) (Perry & Silver, 1982). These data led to the hypothesis that Cd(II) uptake required the PMF and was entering through a Mn(II) transporter. An alternate study found that a *S. aureus mntA* mutant had increased resistance to Cd(II) (Horsburgh *et al.*, 2002). These data have been interpreted to suggest that Cd(II) is transported into *S. aureus* via MntABC (Papp-Wallace & Maguire, 2006), but direct evidence for this is lacking.

Studies using other organisms have provided more convincing data that some metal ion transporters can transport more than one metal. *Escherichia coli* strains over-producing the ZIP family Zn importer ZupT resulted in sensitivity to Fe and Co, as well as cellular accumulation of the metals (Grass *et al.*, 2005). Expression of the *Lactobacillus plantarum* MntA P-type ATPase Mn importer in *E. coli* increased cellular Cd(II) and Mn(II) loads (Hao *et al.*, 1999). Expression of the *sitABCD* in *E. coli* increased cellular Fe and Mn loads (Sabri *et al.*, 2006) and the *Yersinia pestis* YfeABCD metal transporter was shown to transport both Mn and Fe.

Unlike *Streptococcus pneumoniae*, NrdF does not appear to be a primary target of Cu toxicity in *S. aureus*. However, a *S. aureus* strain deficient in synthesizing FeS clusters had increased sensitivity to Cu. Moreover, the addition of Cu resulted in an inability to grow without supplementing the growth medium with the amino acids Leu and Ile, which is a phenotype common to *S. aureus* strains defective in FeS protein maturation (Mashruwala *et al.*, Rosario-Cruz *et al.*, 2015, Mashruwala *et al.*, 2016a). Introduction of the *mntB::tetR* allele corrected both phenotypes suggesting that decreasing Cu influx protects FeS proteins from Cu poisoning. Furthermore, *in vivo* and *in vitro* incubation with Cu(II) inhibited aconitase in a concentration dependent manner. A lower concentration of Cu was necessary to inhibit *in vivo* than needed for inhibition in cell-free lysates. This may be the result of Cu poisoning both the FeS cluster synthesis machinery and holo-AcnA *in vivo* resulting in a compounding effect. Intracellular Cu(I) is a more avid disruptor of AcnA than the Cu(II) (Macomber & Imlay, 2009); however, the inclusion of ascorbic acid to reduce Cu(II) to Cu(I) did not increase AcnA poisoning *in vitro* under the assay conditions utilized. This could be a result of an adequate concentration of molecules in the lysates that can reduce Cu(II). This may result in nullifying the effect of ascorbic acid on Cu(II) reduction. We recently noted a similar effect in the inhibition of AcnA in *Thermus thermophilus*. The concentration of Hg necessary to inhibit AcnA *in vivo* was less than that necessary to inhibit the enzyme in cell lysates (Norambuena *et al.*, 2019).

Similar to the results presented herein, Johnson *et al.* reported the supplementing the medium with Mn protected *Streptococcus pneumoniae* from Cu intoxication (Johnson *et al.*, 2015). We noted that the addition of Mn, at a >10-fold lower concentration than that used by

Johnson *et al.*, protected *S. aureus* against Cu intoxication. This difference could be a result of differing bacterial uptake rates, but these findings led us to hypothesize that the lower amount of Mn required to protect *S. aureus* from Cu intoxication was the result of regulatory effects. Protection in *S. aureus* was dependent upon the presence of the Mn sensing transcriptional regulator MntR. A *cop*- Δ*mntR* strain had increased *mntABC* transcription and decreased growth in the presence of Cu. The decreased growth of the *cop*- Δ*mntR* strain was corrected by the introduction of the *mntA1::Tn* allele. The *cop*- Δ*mntR* strain also had a larger Cu load than the *cop*- strain, and again, this phenotype was mitigated by the introduction of *mntA1::Tn*. These data have led us to modify our working model (Figure 9) wherein Mn protects *S. aureus* against Cu intoxication by binding to MntR resulting in MntR-dependent repression of *mntABC* transcription and ultimately decreasing MntABC-dependent Cu uptake. In light of our findings it would be interesting to examine the effect of the absence of *psaR* and/or *psaBCA* on Cu intoxication in *S. pneumoniae*. We note that there are many variables that may contribute to the differences in the intracellular targets of Cu(II) in *S. pneumonia* and *S. aureus* including growth conditions, growth media utilized and physiology.

To summarize, we have demonstrated that a *S. aureus* strain lacking CopAZ and CopBL is defective in Cu efflux. This strain is protected by loss of function mutations in *mntABC*. *S. aureus* lacking MntABC have decreased cellular copper loads whereas increased transcription of *mntABC* increase Cu loads. We also established that FeS enzymes are a primary target of Cu toxicity. Taken together, these findings expand our understanding of bacterial metal ion homeostasis. Further biochemical studies will be necessary to determine if MntABC can physically import Cu.

Experimental Procedures

Materials and services

Phusion DNA polymerase, deoxynucleoside triphosphates, the quick DNA ligase kit, and restriction enzymes were purchased from New England BioLabs. The plasmid miniprep kit, gel extraction kit, and RNA Protect were purchased from Qiagen. TRIzol and High-Capacity cDNA reverse transcription kits were purchased from Life Technologies. Oligonucleotides, obtained from Integrated DNA Technologies, are listed in Table 2. DNase I was purchased from Ambion. Lysostaphin was purchased from Ambi Products. TSB was purchased from MP Biomedical. Difco BiTek agar was added (15 g L^{-1}) for solid medium. Phosphate buffered saline tablets were purchased from Calbiochem. Distilled and deionized water was used to prepare chemicals, and glassware was often acid washed prior to use. Chelex-100 resin was purchased from Bio-rad. Unless otherwise stated, all chemicals were purchased from Sigma-Aldrich and were of the highest purity obtainable. DNA was sequenced by Genewiz (South Plainfield, NJ).

Bacterial strains, media and growth conditions

Unless specified, the *S. aureus* strains used in this study (Table 1) were isogenic and constructed in the community associated *S. aureus* MRSA strain USA300_LAC that had

cured of the native plasmid pUSA03 that confers erythromycin resistance (Pang *et al.*, 2013).

S. aureus strains were cultured in TSB and grown at 37 °C with shaking at 200 rpm. Unless stated otherwise, cells were cultured in 10- or 30-mL capacity culture tubes containing 1 or 7.5 mL of liquid medium, respectively. The chemically defined minimal medium was described previously and was supplemented with 0.5 μg mL^{-1} lipoic acid (Mashruwala *et al.*, 2016b). Chelex-treated TSB was prepared by incubating liquid TSB overnight at 4 °C with Chelex-100 resin and continuous stirring. The chelated medium was filter sterilized before use. When necessary, antibiotics were added at the final following concentrations: 150 μg mL^{-1} ampicillin (Amp); 30 μg mL^{-1} chloramphenicol (Cm); 10 μg mL^{-1} erythromycin (Erm); 3 μg mL^{-1} tetracycline (Tet); 100 μg mL^{-1} spectinomycin; 150 ng mL^{-1} anhydrotetracycline (Atet). For routine plasmid maintenance, liquid media were supplemented with 10 μg mL^{-1} or 3.3 μg mL^{-1} of chloramphenicol or erythromycin, respectively. The $CuSO_4$ and $MnCl_2$ stocks were prepared in deionized and distilled water and filter sterilized. Liquid phenotypic analysis was conducted in 96-well microtiter plates containing 200 μL of medium per well using a BioTek 808E visible absorption spectrophotometer. Plates were continually shaken at shake speed medium. Culture densities were read at 600 nm. The cells used for inoculation were cultured for 18 hours in TSB medium before washing with PBS. The optical densities (OD) of the cell suspensions were adjusted to 2.5 (A600) in PBS. Two microliters of cells were added to 198 μL of medium. For growth analyses using solid media, strains were cultured for 18 hours in TSB medium before harvesting by centrifugation. Cells were washed with PBS, serial diluted in PBS, and 5 μL aliquots were spotted upon solid media.

Aconitase Enzyme assays

Aconitase (AcnA) assay was conducted as previously described (Mashruwala *et al.*, 2016a). Briefly, Strains were cultured overnight in TSB before washing them with PBS and diluting them to an optical density of 0.05 (A_{600}) in 7.5 mL of chemically defined medium supplemented with 1 % xylose and Cm. Strains were cultured in 30 mL culture tubes for 9 hours. After assaying AcnA, protein concentrations were determined using a copper bicinchoninic acid based colorimetric assay modified for a 96-well plate. Cu inhibition of aconitase was conducted by adding 0–100 μM Cu(II) to cell lysates 20 minutes before assaying activity.

RNA isolation and quantification of mRNA transcripts.

Bacterial strains were cultured for 18 hours in TSB and diluted to a final OD of 0.1 (A_{600}) in 30 mL of fresh TSB or Chelex-treated TSB. The cells were cultured in 250 mL flasks and incubated with shaking till growth reached an OD of 0.8 (A600). One mL was transferred to 10 mL capacity tubes in triplicates and 10 μM $MnCl_2$ final concentration was added to Mn(II) treated group. Both Mn(II) treated and non-treated cultures were then incubated for 30 minutes and harvested. Harvested cells were treated with RNAProtect (Qiagen) for 10 minutes at room temperature, pelleted by centrifugation, and stored at −80 °C. Cell pellets were thawed and washed twice with 0.5 mL of lysis buffer (20 mM RNase-free Sodium acetate, 1 mM EDTA, 0.5 % SDS). The cells were lysed by the addition of 4 μg lysostaphin

and incubated for 40 min at 37 °C until confluent lysis was observed. RNA was isolated using TRIzol reagent according to the manufacturer's instructions. DNA was digested with the Turbo DNA-free kit. The cDNA libraries were constructed using isolated RNA as a template and a High Capacity RNA-to-cDNA kit. An Applied Biosystems StepOnePlus thermocycler and Power SYBR green PCR master mix (Applied Biosystems) were used to quantify DNA abundance. The primer pairs were designed using Primer Express 3.0 software (Applied Biosystems).

Whole cell metal quantification

S. aureus were subcultured in triplicate, from 18 hour grown overnights, to an OD of 0.05 (A_{600}) in 7.5 mL of chelexed TSB in a 30 mL capacity culture tubes. Cultures were incubated with shaking for 8 hrs, before 0–10 μM $CuSO_4$ was added. After 15, 30, or 60 minutes of incubation, samples were transferred into pre-weighted metals free propylene tubes and cells were pelleted by centrifugation using a prechilled table top centrifuge (Eppendorf, Hauppauge, NY). Pellets were washed three times with 10 mL of ice-cold PBS. After decanting the PBS, a fourth spin was conducted to help separate the pellets from any remaining liquid, which was removed using metals free pipettes. Tubes were weighed again to quantify the weight of the cell pellets. All samples were kept at −80 °C or on dry ice until processing.

Cell pellets were acid digested with 2 mL Optima grade nitric acid (ThermoFisher, Waltham, MA) and 500 μL hydrogen peroxide (Sigma, St. Louis, MO) for 24 h at 60 °C. After digestion, 10 mL UltraPure water (Invitrogen, Carlsbad, CA) was added to each sample. Elemental quantification on acid-digested liquid samples was performed using an Agilent 7700 inductively coupled plasma mass spectrometer (Agilent, Santa Clara, CA). The following settings were fixed for the analysis Cell Entrance = −40 V, Cell Exit = −60 V, Plate Bias = −60 V, OctP Bias = −18 V, and collision cell Helium Flow = 4.5 mL min^{-1}. Optimal voltages for Extract 2, Omega Bias, Omega Lens, OctP RF, and Deflect were determined empirically before each sample set was analyzed. Element calibration curves were generated using ARISTAR ICP Standard Mix (VWR). Samples were introduced by peristaltic pump with 0.5 mm internal diameter tubing through a MicroMist borosilicate glass nebulizer (Agilent). Samples were initially up taken at 0.5 rps for 30 seconds followed by 30 seconds at 0.1 rps to stabilize the signal. Samples were analyzed in Spectrum mode at 0.1 rps collecting three points across each peak and performing three replicates of 100 sweeps for each element analyzed. Sampling probe and tubing were rinsed for 20 s at 0.5 rps with 2 % nitric acid between each sample. Data were acquired and analyzed using the Agilent Mass Hunter Workstation Software version A.01.02.

Transposon library construction, mutant selection, and Tn location determination.

The transposon library was constructed in the *cop-* strain as previously described by Grosser et al. (Bae *et al.*, 2004, Grosser *et al.*, 2018). Briefly, pMG020 (harboring transposase) was freshly transformed into RN4220 and plated and incubated on TSA Tet (10 μg/mL) at 30 °C. Single colonies were selected and grown in TSB Tet (10 μg mL^{-1}) at 30 °C and lysates were generated. The *cop-* strain carrying pBursa was transduced with pMG020 and selected with TSA-Cm-Tet at 30 °C. Individual colonies were struck on Cm-Tet plates. Individual colonies

were suspended in 200 μL sterile water and 15 μL aliquots were spread onto TSA plates containing 10 μg mL^{-1} Erm and incubated at 43 °C for 24 hours to allow for transposition. In total, colonies from 170 Petri plates containing approximately 3000 colonies each were pooled using TSB 10 μg mL^{-1} Erm with 25 % glycerol. Aliquots were thoroughly mixed by vortexing and combined into a single pool of transposon mutants. This mutant library was cultured for 2 hours with shaking at 43 °C before 1 mL aliquots were frozen and stored at −80 °C. An aliquot of the *cop*- Tn library was plated on TSA plates containing 2.5 mM $CuSO_4$ to select for Cu resistant mutants. Strains were further studied after reconstruction and phenotypic verification.

The protocol outlined by Fey et al. was used to determine the locations of transposon insertions (Fey *et al.*, 2013). Briefly, chromosomal DNA was digested using AciI and the resulting DNA fragments were ligated using quick ligase kit and PCR reactions were performed using the Tn buster and Martn-ermR primers. The PCR products were gel purified and sequenced to identify the transposon genome junction sites.

Recombinant DNA and genetic techniques

JMB1100 chromosomal DNA was used as a template for PCR reactions. *Escherichia coli* PX5α (Protein Express) was used as a cloning host and for plasmid propagation. Plasmids were isolated and transformed into *S. aureus* strain RN4220 using standard protocol (Grosser & Richardson, 2016) and were conducted using phage 80α (Novick, 1991). All strains were verified by PCR and/or sequencing.

Creation of plasmids and mutant strains

Construction of plasmids for mutant generation or genetic complementation was done using yeast homologous recombination cloning as previously outlined (Mashruwala & Boyd, 2015, Joska *et al.*, 2014). The following primer pairs were used to create the amplicons necessary to make pJB38_Δ*copAZ*: Ycc Pjb38 for and YCC CopAZ rev; CopAZ Up for and copAZ up rev; copAZ dwn for and pJB38 copAZ rev. The amplified PCR fragments were combined with EcoRI linearized pJB38 plasmid and transformed into competent *Saccharomyces cerevisiae* FY2. To create pEPSA_*mntABC*, pEPSA5_*citB_FLAG* (Mashruwala *et al.*, 2015) was linearized with NheI and MluI. The *mntABC* insert was amplified using primers pEPmntABCfor and mntABCYCCrev, combined with vector, and transformed into competent *Saccharomyces cerevisiae* FY2For all *tetR* insertion mutants, the tetracycline cassette was amplified from strain JMB1432. The pJB38_*rsaE::tetR* was used as a backbone to create the pJB38_*mnt* plasmids. To generate the pJB38_*rseA::tetR*, pJB38 was linearized with EcoRI and combined with PCR amplicons generated using the following primer pairs: pJB39_yCC forward and Ycc rseA rev; Ycc rseA for and rseA tetR rev; rseA tetR for and tetR rseA rev; tetR rseA for and rseA pJB38 rev

To generate all *mnt* and *rsaC* pJB38 vectors, pJB38_Δ*rsaE::tetR* was linearized using NheI and MluI. The gel purified vector was then combined with amplicons and transformed into competent *Saccharomyces cerevisiae* FY2. The following primer pairs were used to create the amplicons necessary to make pJB38_*ΔmntR::tetR*: YccmntRfor and mntRtetRrev; tetRmntRfor and pJB38mntRrev. The following primer pairs were used to create the

amplicons necessary to make pJB38_*ΔmntA::tetR*: YCCmntAfor and mntAtetRrev; mntAtetRfor and tetRmntArev; tetRmntAfor and pJB38mntArev. The following primer pairs were used to create the amplicons necessary to make pJB38_*ΔmntB::tetR*: YCCmntBfor and mntBtetRrev; mntBtetRfor and tetRmntBrev; tetRmntBfor and pJB38mntArev. The following primer pairs were used to create the amplicons necessary to make pJB38_*ΔmntAB::tetR*: YCCmntAfor and mntAtetRrev; mntAtetRfor and tetRmntABrev; tetRmntABfor and pJB38mntArev. The following primer pairs were used to create the amplicons necessary to make pJB38_Δ*mntABC*::*tetR*: YCCmntABCfor and mntABCtetRrev; mntABCtetRfor and tetRmntABCrev; tetRmntABCfor and pJB38mntABCrev. The following primer pairs were used to create pJB38_*ΔrsaC::tetR*: YCCrsaCfor and tetupRsaCrev; upRsaCtetfwd and downRsaCtetrev; tetdownRsaCfwd and pJB38rsaCrev. The following primer pairs were used to create the amplicons necessary to make pLL39_*mntABC*: pLLYCC5 and mntABCYCC3; YccmntABC and mntABCpLL39. The pLL39 vector was linearized with SalI, combined with PCR amplicons, and transformed into *Saccharomyces cerevisiae* FY2. The *pLL39_ mntABC* construct was transformed into RN4220 containing pLL2787 and integrated onto the chromosome at the Φ11 *attB* site as previously described (Roberts *et al.*, 2017). Episome integration was verified using the Scv8 and Scv9 primers. The pML vectors were created by linearizing pML using EcoRI and SalI and was ligated with similarly digested amplicons. The following primer pairs were used to generate the amplicons for the pML100_*rsaC* and pML100_*rsaC* antisense clones, respectively: RsaCSalIsense and RsaCEcoRIsense; RsaCSalIantisense and RsaCEcoRIantisense.

Mutant strains were constructed using the pJB38 allelic exchange vectors as described previously (Rosario-Cruz *et al.*, 2015). The *cop*- strain was created using the Δ*copBL* mutant strain (JMB7901) (ΔSAUSA300_0078–0079) and pJB38_Δ*copAZ*.

Supplementary Material

Refer to Web version on PubMed Central for supplementary material.

Acknowledgements:

The Boyd lab is funded by NIAID award 1R01AI139100-01, NSF award MCB-1750624, and USDA MRF project NE-1028.

References

Achard ME, Stafford SL, Bokil NJ, Chartres J, Bernhardt PV, Schembri MA, Sweet MJ, and McEwan AG (2012) Copper redistribution in murine macrophages in response to *Salmonella* infection. Biochem J 444: 51–57. [PubMed: 22369063]

Andreini C, Banci L, Bertini I, and Rosato A (2008) Occurrence of copper proteins through the three domains of life: a bioinformatic approach. Journal of proteome research 7: 209–216. [PubMed: 17988086]

Anjem A, and Imlay JA (2012) Mononuclear iron enzymes are primary targets of hydrogen peroxide stress. J Biol Chem 287: 15544–15556. [PubMed: 22411989]

Arguello JM, Eren E, and Gonzalez-Guerrero M (2007) The structure and function of heavy metal transport P1B-ATPases. Biometals 20: 233–248. [PubMed: 17219055]

Bae T, Banger AK, Wallace A, Glass EM, Aslund F, Schneewind O, and Missiakas DM (2004) *Staphylococcus aureus* virulence genes identified by bursa aurealis mutagenesis and nematode killing. Proc Natl Acad Sci U S A 101: 12312–12317. [PubMed: 15304642]

Bae T, Glass EM, Schneewind O, and Missiakas D (2008) Generating a collection of insertion mutations in the *Staphylococcus aureus* genome using bursa aurealis. Methods Mol Biol 416: 103–116. [PubMed: 18392963]

Baker J, Sitthisak S, Sengupta M, Johnson M, Jayaswal RK, and Morrissey JA (2010) Copper stress induces a global stress response in *Staphylococcus aureus* and represses sae and agr expression and biofilm formation. Appl Environ Microbiol 76: 150–160. [PubMed: 19880638]

Banci L, Bertini I, Del Conte R, Markey J, and Ruiz-Duenas FJ (2001) Copper trafficking: the solution structure of *Bacillus subtilis* CopZ. Biochemistry 40: 15660–15668. [PubMed: 11747441]

Becker KW, and Skaar EP (2014) Metal limitation and toxicity at the interface between host and pathogen. FEMS microbiology reviews 38: 1235–1249. [PubMed: 25211180]

Begg SL (2019) The role of metal ions in the virulence and viability of bacterial pathogens. Biochem Soc Trans 47: 77–87. [PubMed: 30626704]

Beinert H, Kennedy MC, and Stout CD (1996) Aconitase as iron-sulfur protein, enzyme, and iron-regulatory protein. Chemical reviews 96: 2335–2373. [PubMed: 11848830]

Beveridge SJ, Garrett IR, Whitehouse MW, Vernon-Roberts B, and Brooks PM (1985) Biodistribution of 64Cu in inflamed rats following administration of two anti-inflammatory copper complexes. Agents Actions 17: 104–111. [PubMed: 3878667]

Borremans B, Hobman JL, Provoost A, Brown NL, and van Der Lelie D (2001) Cloning and functional analysis of the *pbr* lead resistance determinant of *Ralstonia metallidurans* CH34. J Bacteriol 183: 5651–5658. [PubMed: 11544228]

Bose JL, Fey PD, and Bayles KW (2013) Genetic tools to enhance the study of gene function and regulation in *Staphylococcus aureus*. Appl Environ Microbiol 79: 2218–2224. [PubMed: 23354696]

Brancaccio D, Gallo A, Piccioli M, Novellino E, Ciofi-Baffoni S, and Banci L (2017) [4Fe-4S] Cluster Assembly in Mitochondria and Its Impairment by Copper. J Am Chem Soc 139: 719–730. [PubMed: 27989128]

Chandrangsu P, and Helmann JD (2016) Intracellular Zn(II) Intoxication Leads to Dysregulation of the PerR Regulon Resulting in Heme Toxicity in *Bacillus subtilis*. PLoS Genet 12: e1006515. [PubMed: 27935957]

Chandrangsu P, Rensing C, and Helmann JD (2017) Metal homeostasis and resistance in bacteria. Nat Rev Microbiol 15: 338–350. [PubMed: 28344348]

Chillappagari S, Seubert A, Trip H, Kuipers OP, Marahiel MA, and Miethke M (2010) Copper stress affects iron homeostasis by destabilizing iron-sulfur cluster formation in *Bacillus subtilis*. J Bacteriol 192: 2512–2524. [PubMed: 20233928]

Claverys JP (2001) A new family of high-affinity ABC manganese and zinc permeases. Res Microbiol 152: 231–243. [PubMed: 11421271]

Cotruvo JA Jr., and Stubbe J (2012) Metallation and mismetallation of iron and manganese proteins in vitro and in vivo: the class I ribonucleotide reductases as a case study. Metallomics : integrated biometal science 4: 1020–1036. [PubMed: 22991063]

Counago RM, Ween MP, Begg SL, Bajaj M, Zuegg J, O'Mara ML, Cooper MA, McEwan AG, Paton JC, Kobe B, and McDevitt CA (2014) Imperfect coordination chemistry facilitates metal ion release in the Psa permease. Nat Chem Biol 10: 35–41. [PubMed: 24212134]

Dintilhac A, Alloing G, Granadel C, and Claverys JP (1997) Competence and virulence of *Streptococcus pneumoniae*: Adc and PsaA mutants exhibit a requirement for Zn and Mn resulting from inactivation of putative ABC metal permeases. Mol Microbiol 25: 727–739. [PubMed: 9379902]

Djoko KY, and McEwan AG (2013) Antimicrobial action of copper is amplified via inhibition of heme biosynthesis. ACS Chem Biol 8: 2217–2223. [PubMed: 23895035]

Dollwet HH, and Sorenson JR, (1985) Historic uses of copper compounds in medicine, p. 80–87. Humana Press Inc., Arkansas.

Ekici S, Yang H, Koch HG, and Daldal F (2012) Novel transporter required for biogenesis of cbb3-type cytochrome c oxidase in *Rhodobacter capsulatus*. mBio 3.

Fey PD, Endres JL, Yajjala VK, Widhelm TJ, Boissy RJ, Bose JL, and Bayles KW (2013) A genetic resource for rapid and comprehensive phenotype screening of nonessential *Staphylococcus aureus* genes. mBio 4: e00537–00512. [PubMed: 23404398]

Forsyth RA, Haselbeck RJ, Ohlsen KL, Yamamoto RT, Xu H, Trawick JD, Wall D, Wang L, Brown-Driver V, Froelich JM, C KG, King P, McCarthy M, Malone C, Misiner B, Robbins D, Tan Z, Zhu Zy ZY, Carr G, Mosca DA, Zamudio C, Foulkes JG, and Zyskind JW (2002) A genome-wide strategy for the identification of essential genes in *Staphylococcus aureus*. Mol Microbiol 43: 1387–1400. [PubMed: 11952893]

Gaballa A, and Helmann JD (2003) *Bacillus subtilis* CPx-type ATPases: characterization of Cd, Zn, Co and Cu efflux systems. Biometals 16: 497–505. [PubMed: 12779235]

Gardner PR, and Fridovich I (1991) Superoxide sensitivity of the *Escherichia coli* aconitase. Journal of Biological Chemistry 266: 19328–19333.

Glasfeld A, Guedon E, Helmann JD, and Brennan RG (2003) Structure of the manganese-bound manganese transport regulator of *Bacillus subtilis*. Nat Struct Biol 10: 652–657. [PubMed: 12847518]

Grass G, Franke S, Taudte N, Nies DH, Kucharski LM, Maguire ME, and Rensing C (2005) The metal permease ZupT from *Escherichia coli* is a transporter with a broad substrate spectrum. J Bacteriol 187: 1604–1611. [PubMed: 15716430]

Grass G, Rensing C, and Solioz M (2011) Metallic copper as an antimicrobial surface. Appl Environ Microbiol 77: 1541–1547. [PubMed: 21193661]

Gribenko A, Mosyak L, Ghosh S, Parris K, Svenson K, Moran J, Chu L, Li S, Liu T, Woods VL Jr., Jansen KU, Green BA, Anderson AS, and Matsuka YV (2013) Three-dimensional structure and biophysical characterization of *Staphylococcus aureus* cell surface antigen-manganese transporter MntC. J Mol Biol 425: 3429–3445. [PubMed: 23827136]

Grosser MR, Paluscio E, Thurlow LR, Dillon MM, Cooper VS, Kawula TH, and Richardson AR (2018) Genetic requirements for *Staphylococcus aureus* nitric oxide resistance and virulence. PLoS Pathog 14: e1006907. [PubMed: 29554137]

Grosser MR, and Richardson AR (2016) Method for Preparation and Electroporation of *S. aureus* and *S. epidermidis*. Methods Mol Biol 1373: 51–57. [PubMed: 25966876]

Grossoehme N, Kehl-Fie TE, Ma Z, Adams KW, Cowart DM, Scott RA, Skaar EP, and Giedroc DP (2011) Control of copper resistance and inorganic sulfur metabolism by paralogous regulators in *Staphylococcus aureus*. J Biol Chem 286: 13522–13531. [PubMed: 21339296]

Gu M, and Imlay JA (2013) Superoxide poisons mononuclear iron enzymes by causing mismetallation. Mol Microbiol 89: 123–134. [PubMed: 23678969]

Guan G, Pinochet-Barros A, Gaballa A, Patel SJ, Arguello JM, and Helmann JD (2015) PfeT, a P1B4 -type ATPase, effluxes ferrous iron and protects *Bacillus subtilis* against iron intoxication. Mol Microbiol 98: 787–803. [PubMed: 26261021]

Gupta A, Matsui K, Lo JF, and Silver S (1999) Molecular basis for resistance to silver cations in *Salmonella*. Nature medicine 5: 183–188.

Handke LD, Hawkins JC, Miller AA, Jansen KU, and Anderson AS (2013) Regulation of *Staphylococcus aureus* MntC expression and its role in response to oxidative stress. PLoS One 8: e77874. [PubMed: 24205007]

Hao Z, Chen S, and Wilson DB (1999) Cloning, expression, and characterization of cadmium and manganese uptake genes from *Lactobacillus plantarum*. Appl Environ Microbiol 65: 4746–4752. [PubMed: 10543781]

Hodgkinson V, and Petris MJ (2012) Copper homeostasis at the host-pathogen interface. J Biol Chem 287: 13549–13555. [PubMed: 22389498]

Horsburgh MJ, Ingham E, and Foster SJ (2001) In *Staphylococcus aureus*, Fur is an interactive regulator with PerR, contributes to virulence, and Is necessary for oxidative stress resistance through positive regulation of catalase and iron homeostasis. J Bacteriol 183: 468–475. [PubMed: 11133939]

Horsburgh MJ, Wharton SJ, Cox AG, Ingham E, Peacock S, and Foster SJ (2002) MntR modulates expression of the PerR regulon and superoxide resistance in *Staphylococcus aureus* through control of manganese uptake. Mol Microbiol 44: 1269–1286. [PubMed: 12028379]

Huang X, Shin JH, Pinochet-Barros A, Su TT, and Helmann JD (2017) *Bacillus subtilis* MntR coordinates the transcriptional regulation of manganese uptake and efflux systems. Mol Microbiol 103: 253–268. [PubMed: 27748968]

Imlay JA (2014) The mismetallation of enzymes during oxidative stress. J Biol Chem 289: 28121–28128. [PubMed: 25160623]

Jaroslawiecka A, and Piotrowska-Seget Z (2014) Lead resistance in micro-organisms. Microbiology 160: 12–25. [PubMed: 24124204]

Johnson MD, Kehl-Fie TE, and Rosch JW (2015) Copper intoxication inhibits aerobic nucleotide synthesis in *Streptococcus pneumoniae*. Metallomics : integrated biometal science 7: 786–794. [PubMed: 25730343]

Johnston JW, Briles DE, Myers LE, and Hollingshead SK (2006) Mn2+-dependent regulation of multiple genes in *Streptococcus pneumoniae* through PsaR and the resultant impact on virulence. Infect Immun 74: 1171–1180. [PubMed: 16428766]

Joska TM, Mashruwala A, Boyd JM, and Belden WJ (2014) A universal cloning method based on yeast homologous recombination that is simple, efficient, and versatile. J Microbiol Methods 100: 46–51. [PubMed: 24418681]

Kehl-Fie TE, Zhang Y, Moore JL, Farrand AJ, Hood MI, Rathi S, Chazin WJ, Caprioli RM, and Skaar EP (2013) MntABC and MntH contribute to systemic *Staphylococcus aureus* infection by competing with calprotectin for nutrient manganese. Infect Immun 81: 3395–3405. [PubMed: 23817615]

Kim J, Senadheera DB, Levesque CM, and Cvitkovitch DG (2012) TcyR regulates L-cystine uptake via the TcyABC transporter in *Streptococcus mutans*. FEMS Microbiol Lett 328: 114–121. [PubMed: 22212096]

Kreiswirth BN, Lofdahl S, Betley MJ, O'Reilly M, Schlievert PM, Bergdoll MS, and Novick RP (1983) The toxic shock syndrome exotoxin structural gene is not detectably transmitted by a prophage. Nature 305: 709–712. [PubMed: 6226876]

Laddaga RA, and Silver S (1985) Cadmium uptake in *Escherichia coli* K-12. J Bacteriol 162: 1100–1105. [PubMed: 3888954]

Ladomersky E, Khan A, Shanbhag V, Cavet JS, Chan J, Weisman GA, and Petris MJ (2017) Host and Pathogen Copper-Transporting P-Type ATPases Function Antagonistically during *Salmonella* Infection. Infect Immun 85.

Lalaouna D, Baude J, Wu Z, Tomasini A, Chicher J, Marzi S, Vandenesch F, Romby P, Caldelari I, and Moreau K (2019) RsaC sRNA modulates the oxidative stress response of *Staphylococcus aureus* during manganese starvation. Nucleic Acids Res 47: 9871–9887. [PubMed: 31504767]

Lei MG, Cue D, Roux CM, Dunman PM, and Lee CY (2011) Rsp inhibits attachment and biofilm formation by repressing *fnbA* in *Staphylococcus aureus* MW2. J Bacteriol 193: 5231–5241. [PubMed: 21804010]

Li N, Yang XY, Guo Z, Zhang J, Cao K, Han J, Zhang G, Liu L, Sun X, and He QY (2014) Varied metal-binding properties of lipoprotein PsaA in *Streptococcus pneumoniae*. J Biol Inorg Chem 19: 829–838. [PubMed: 24553956]

Lim KH, Jones CE, vanden Hoven RN, Edwards JL, Falsetta ML, Apicella MA, Jennings MP, and McEwan AG (2008) Metal binding specificity of the MntABC permease of *Neisseria gonorrhoeae* and its influence on bacterial growth and interaction with cervical epithelial cells. Infect Immun 76: 3569–3576. [PubMed: 18426887]

Lisher JP, Higgins KA, Maroney MJ, and Giedroc DP (2013) Physical characterization of the manganese-sensing pneumococcal surface antigen repressor from *Streptococcus pneumoniae*. Biochemistry 52: 7689–7701. [PubMed: 24067066]

Luong TT, and Lee CY (2007) Improved single-copy integration vectors for *Staphylococcus aureus*. J Microbiol Methods 70: 186–190. [PubMed: 17512993]

Ma Z, Cowart DM, Scott RA, and Giedroc DP (2009) Molecular insights into the metal selectivity of the copper(I)-sensing repressor CsoR from *Bacillus subtilis*. Biochemistry 48: 3325–3334. [PubMed: 19249860]

Macomber L, and Imlay JA (2009) The iron-sulfur clusters of dehydratases are primary intracellular targets of copper toxicity. Proc Natl Acad Sci U S A 106: 8344–8349. [PubMed: 19416816]

Malachowa N, and DeLeo FR (2010) Mobile genetic elements of *Staphylococcus aureus*. Cell Mol Life Sci 67: 3057–3071. [PubMed: 20668911]

Martin JE, and Imlay JA (2011) The alternative aerobic ribonucleotide reductase of *Escherichia coli*, NrdEF, is a manganese-dependent enzyme that enables cell replication during periods of iron starvation. Mol Microbiol 80: 319–334. [PubMed: 21338418]

Mashruwala AA, Bhatt S, Poudel S, Boyd ES, and Boyd JM (2016a) The DUF59 Containing Protein SufT Is Involved in the Maturation of Iron-Sulfur (FeS) Proteins during Conditions of High FeS Cofactor Demand in *Staphylococcus aureus*. PLoS Genet 12: e1006233. [PubMed: 27517714]

Mashruwala AA, and Boyd JM (2015) De Novo Assembly of Plasmids Using Yeast Recombinational Cloning. Methods Mol Biol 1373: 33–41.

Mashruwala AA, and Boyd JM (2017) The *Staphylococcus aureus* SrrAB Regulatory System Modulates Hydrogen Peroxide Resistance Factors, Which Imparts Protection to Aconitase during Aerobic Growth. PLoS One 12: e0170283. [PubMed: 28099473]

Mashruwala AA, Pang YY, Rosario-Cruz Z, Chahal HK, Benson MA, Mike LA, Skaar EP, Torres VJ, Nauseef WM, and Boyd JM Nfu facilitates the maturation of iron-sulfur proteins and participates in virulence in *Staphylococcus aureus*. Mol Microbiol 95: 383–409. [PubMed: 25388433]

Mashruwala AA, Pang YY, Rosario-Cruz Z, Chahal HK, Benson MA, Mike LA, Skaar EP, Torres VJ, Nauseef WM, and Boyd JM (2015) Nfu facilitates the maturation of iron-sulfur proteins and participates in virulence in *Staphylococcus aureus*. Mol Microbiol 95: 383–409. [PubMed: 25388433]

Mashruwala AA, Roberts CA, Bhatt S, May KL, Carroll RK, Shaw LN, and Boyd JM (2016b) *Staphylococcus aureus* SufT: An essential iron-sulfur cluster assembly factor in cells experiencing a high-demand for lipoic acid. Mol Microbiol.

McAllister LJ, Tseng HJ, Ogunniyi AD, Jennings MP, McEwan AG, and Paton JC (2004) Molecular analysis of the *psa* permease complex of *Streptococcus pneumoniae*. Mol Microbiol 53: 889–901. [PubMed: 15255900]

McDevitt CA, Ogunniyi AD, Valkov E, Lawrence MC, Kobe B, McEwan AG, and Paton JC (2011) A molecular mechanism for bacterial susceptibility to zinc. PLoS Pathog 7: e1002357. [PubMed: 22072971]

Moore CM, Gaballa A, Hui M, Ye RW, and Helmann JD (2005) Genetic and physiological responses of *Bacillus subtilis* to metal ion stress. Mol Microbiol 57: 27–40. [PubMed: 15948947]

Ngamchuea K, Batchelor-McAuley C, and Compton RG (2016) The Copper(II)-Catalyzed Oxidation of Glutathione. Chemistry 22: 15937–15944. [PubMed: 27649691]

Norambuena J, Hanson TE, Barkay T, and Boyd JM (2019) Superoxide Dismutase and Pseudocatalase Increase Tolerance to Hg(II) in *Thermus thermophilus* HB27 by Maintaining the Reduced Bacillithiol Pool. mBio 10.

Norambuena J, Wang Y, Hanson T, Boyd JM, and Barkay T (2017) Low molecular weight thiols and thioredoxins are important players in Hg(II) resistance in *Thermus thermophilus* HB27. Appl Environ Microbiol.

Novak R, Braun JS, Charpentier E, and Tuomanen E (1998) Penicillin tolerance genes of *Streptococcus pneumoniae*: the ABC-type manganese permease complex Psa. Mol Microbiol 29: 1285–1296. [PubMed: 9767595]

Novick RP (1991) Genetic systems in staphylococci. Methods Enzymol 204: 587–636. [PubMed: 1658572]

Palmer LD, and Skaar EP (2016) Transition Metals and Virulence in Bacteria. Annu Rev Genet 50: 67–91. [PubMed: 27617971]

Pang YY, Schwartz J, Bloomberg S, Boyd JM, Horswill AR, and Nauseef WM (2013) Methionine Sulfoxide Reductases Protect against Oxidative Stress in *Staphylococcus aureus* Encountering Exogenous Oxidants and Human Neutrophils. J Innate Immun.

Papp-Wallace KM, and Maguire ME (2006) Manganese transport and the role of manganese in virulence. Annual review of microbiology 60: 187–209.

Perry RD, and Silver S (1982) Cadmium and manganese transport in *Staphylococcus aureus* membrane vesicles. J Bacteriol 150: 973–976. [PubMed: 7068540]

Purves J, Thomas J, Riboldi GP, Zapotoczna M, Tarrant E, Andrew PW, Londono A, Planet PJ, Geoghegan JA, Waldron KJ, and Morrissey JA (2018) A horizontally gene transferred copper resistance locus confers hyper-resistance to antibacterial copper toxicity and enables survival of community acquired methicillin resistant *Staphylococcus aureus* USA300 in macrophages. Environmental microbiology 20: 1576–1589. [PubMed: 29521441]

Que Q, and Helmann JD (2000) Manganese homeostasis in *Bacillus subtilis* is regulated by MntR, a bifunctional regulator related to the diphtheria toxin repressor family of proteins. Mol Microbiol 35: 1454–1468. [PubMed: 10760146]

Quintana J, Novoa-Aponte L, and Arguello JM (2017) Copper homeostasis networks in the bacterium *Pseudomonas aeruginosa*. J Biol Chem 292: 15691–15704. [PubMed: 28760827]

Rabinovitch I, Yanku M, Yeheskel A, Cohen G, Borovok I, and Aharonowitz Y (2010) *Staphylococcus aureus* NrdH redoxin is a reductant of the class Ib ribonucleotide reductase. J Bacteriol 192: 4963–4972. [PubMed: 20675493]

Rigo A, Corazza A, di Paolo ML, Rossetto M, Ugolini R, and Scarpa M (2004) Interaction of copper with cysteine: stability of cuprous complexes and catalytic role of cupric ions in anaerobic thiol oxidation. Journal of inorganic biochemistry 98: 1495–1501. [PubMed: 15337601]

Roberts CA, Al-Tameemi HM, Mashruwala AA, Rosario-Cruz Z, Chauhan U, Sause WE, Torres VJ, Belden WJ, and Boyd JM (2017) The Suf iron-sulfur cluster biosynthetic system is essential in *Staphylococcus aureus* and decreased Suf function results in global metabolic defects and reduced survival in human neutrophils. Infect Immun.

Rosario-Cruz Z, Chahal HK, Mike LA, Skaar EP, and Boyd JM (2015) Bacillithiol has a role in Fe-S cluster biogenesis in *Staphylococcus aureus*. Mol Microbiol 98: 218–242. [PubMed: 26135358]

Rosario-Cruz Z, Eletsky A, Daigham NS, Al-Tameemi H, Swapna GVT, Kahn PC, Szyperski T, Montelione GT, and Boyd JM (2019) The *copBL* operon protects *Staphylococcus aureus* from copper toxicity: CopL is an extracellular membrane-associated copper-binding protein. J Biol Chem 294: 4027–4044. [PubMed: 30655293]

Sabri M, Leveille S, and Dozois CM (2006) A SitABCD homologue from an avian pathogenic *Escherichia coli* strain mediates transport of iron and manganese and resistance to hydrogen peroxide. Microbiology 152: 745–758. [PubMed: 16514154]

Scarpa M, Momo F, Viglino P, and Rigo A (1996) Activated oxygen species in the oxidation of glutathione A kinetic study. Biophysical Chemistry 60: 53–61.

Shafeeq S, Yesilkaya H, Kloosterman TG, Narayanan G, Wandel M, Andrew PW, Kuipers OP, and Morrissey JA (2011) The *cop* operon is required for copper homeostasis and contributes to virulence in *Streptococcus pneumoniae*. Mol Microbiol 81: 1255–1270. [PubMed: 21736642]

Singleton C, Hearnshaw S, Zhou L, Le Brun NE, and Hemmings AM (2009) Mechanistic insights into Cu(I) cluster transfer between the chaperone CopZ and its cognate Cu(I)-transporting P-type ATPase, CopA. Biochem J 424: 347–356. [PubMed: 19751213]

Sitthisak S, Knutsson L, Webb JW, and Jayaswal RK (2007) Molecular characterization of the copper transport system in *Staphylococcus aureus*. Microbiology 153: 4274–4283. [PubMed: 18048940]

Somerville GA, Chaussee MS, Morgan CI, Fitzgerald JR, Dorward DW, Reitzer LJ, and Musser JM (2002) *Staphylococcus aureus* aconitase inactivation unexpectedly inhibits post-exponential-phase growth and enhances stationary-phase survival. Infect Immun 70: 6373–6382. [PubMed: 12379717]

Tan G, Cheng Z, Pang Y, Landry AP, Li J, Lu J, and Ding H (2014) Copper binding in IscA inhibits iron-sulphur cluster assembly in *Escherichia coli*. Mol Microbiol 93: 629–644. [PubMed: 24946160]

Tan G, Yang J, Li T, Zhao J, Sun S, Li X, Lin C, Li J, Zhou H, Lyu J, and Ding H (2017) Anaerobic Copper Toxicity and Iron-Sulfur Cluster Biogenesis in *Escherichia coli*. Appl Environ Microbiol 83.

Tarrant E, G PR, McIlvin MR, Stevenson J, Barwinska-Sendra A, Stewart LJ, Saito MA, and Waldron KJ (2019) Copper stress in *Staphylococcus aureus* leads to adaptive changes in central carbon metabolism. Metallomics : integrated biometal science 11: 183–200. [PubMed: 30443649]

Tenover FC, McDougal LK, Goering RV, Killgore G, Projan SJ, Patel JB, and Dunman PM (2006) Characterization of a strain of community-associated methicillin-resistant *Staphylococcus aureus* widely disseminated in the United States. J Clin Microbiol 44: 108–118. [PubMed: 16390957]

Tottey S, Rich PR, Rondet SA, and Robinson NJ (2001) Two Menkes-type atpases supply copper for photosynthesis in *Synechocystis* PCC 6803. J Biol Chem 276: 19999–20004. [PubMed: 11264284]

Turner NA, Sharma-Kuinkel BK, Maskarinec SA, Eichenberger EM, Shah PP, Carugati M, Holland TL, and Fowler VG Jr. (2019) Methicillin-resistant *Staphylococcus aureus*: an overview of basic and clinical research. Nat Rev Microbiol 17: 203–218. [PubMed: 30737488]

Tynecka Z, Gos Z, and Zajac J (1981) Reduced cadmium transport determined by a resistance plasmid in *Staphylococcus aureus*. J Bacteriol 147: 305–312. [PubMed: 7263608]

Wagner D, Maser J, Lai B, Cai Z, Barry CE 3rd, Honer Zu Bentrup K, Russell DG, and Bermudez LE (2005) Elemental analysis of *Mycobacterium avium*-, *Mycobacterium tuberculosis*-, and *Mycobacterium smegmatis*-containing phagosomes indicates pathogen-induced microenvironments within the host cell's endosomal system. J Immunol 174: 1491–1500. [PubMed: 15661908]

Waldron KJ, and Robinson NJ (2009) How do bacterial cells ensure that metalloproteins get the correct metal? Nat Rev Microbiol 7: 25–35. [PubMed: 19079350]

White C, Lee J, Kambe T, Fritsche K, and Petris MJ (2009) A role for the ATP7A copper-transporting ATPase in macrophage bactericidal activity. J Biol Chem 284: 33949–33956. [PubMed: 19808669]

Wilkens S (2015) Structure and mechanism of ABC transporters. F1000Prime Rep 7: 14. [PubMed: 25750732]

Xu FF, and Imlay JA (2012) Silver(I), mercury(II), cadmium(II), and zinc(II) target exposed enzymic iron-sulfur clusters when they toxify *Escherichia coli*. Appl Environ Microbiol 78: 3614–3621. [PubMed: 22344668]

Zapotoczna M, Riboldi GP, Moustafa AM, Dickson E, Narechania A, Morrissey JA, Planet PJ, Holden MTG, Waldron KJ, and Geoghegan JA (2018) Mobile-Genetic-Element-Encoded Hypertolerance to Copper Protects *Staphylococcus aureus* from Killing by Host Phagocytes. mBio 9.

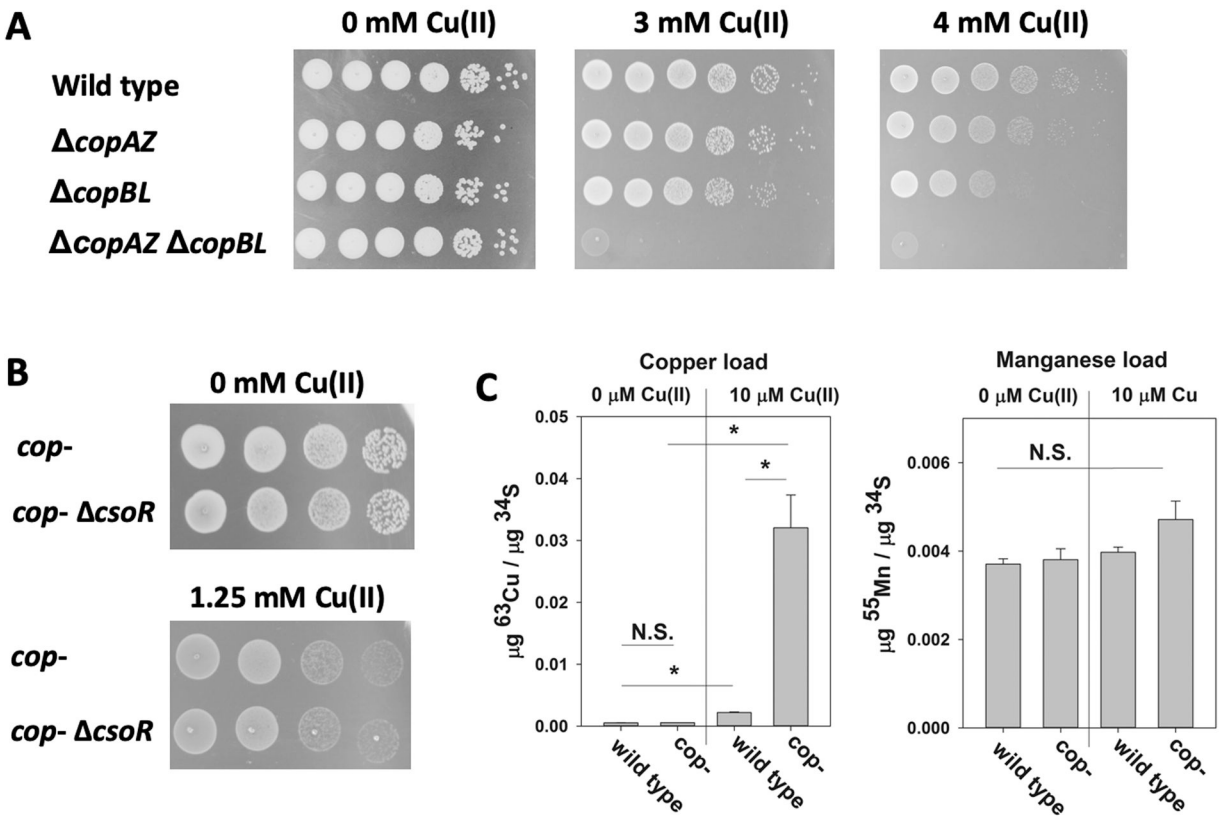

Figure 1. *S. aureus* CopBL and CopAZ function in copper detoxification.

Panel A; Spot plate analysis of wild-type (JMB1100), Δ*copAZ* (JMB8571), Δ*copBL* (JMB7901), Δ*copAZ* Δ*copBL* (*cop-*) (JMB8573). Overnight cultures were serial diluted and spot plated on TSB medium containing various concentrations of Cu. Panel B; Spot plate analysis of *cop-* (JMB8573) and *cop- csoR::Tn* (JMB8723). Overnight cultures were serial diluted and spot plated on TSB medium with and without 1.25 mM Cu. Panel C; Total cellular ^{63}Cu and ^{55}Mn loads were determined in the WT and *cop-* strains using inductively coupled plasma mass spectrometry after growth in TSB medium in the presence and absence of 10 μM Cu. The data represent the mean of three biological replicates and errors are presented as standard deviations. Paired student t-tests were performed on the samples and N.S. denotes not significant ($p > 0.1$) and * denotes $p \leq 0.05$. Photos from representative experiments are shown in Panels A and B.

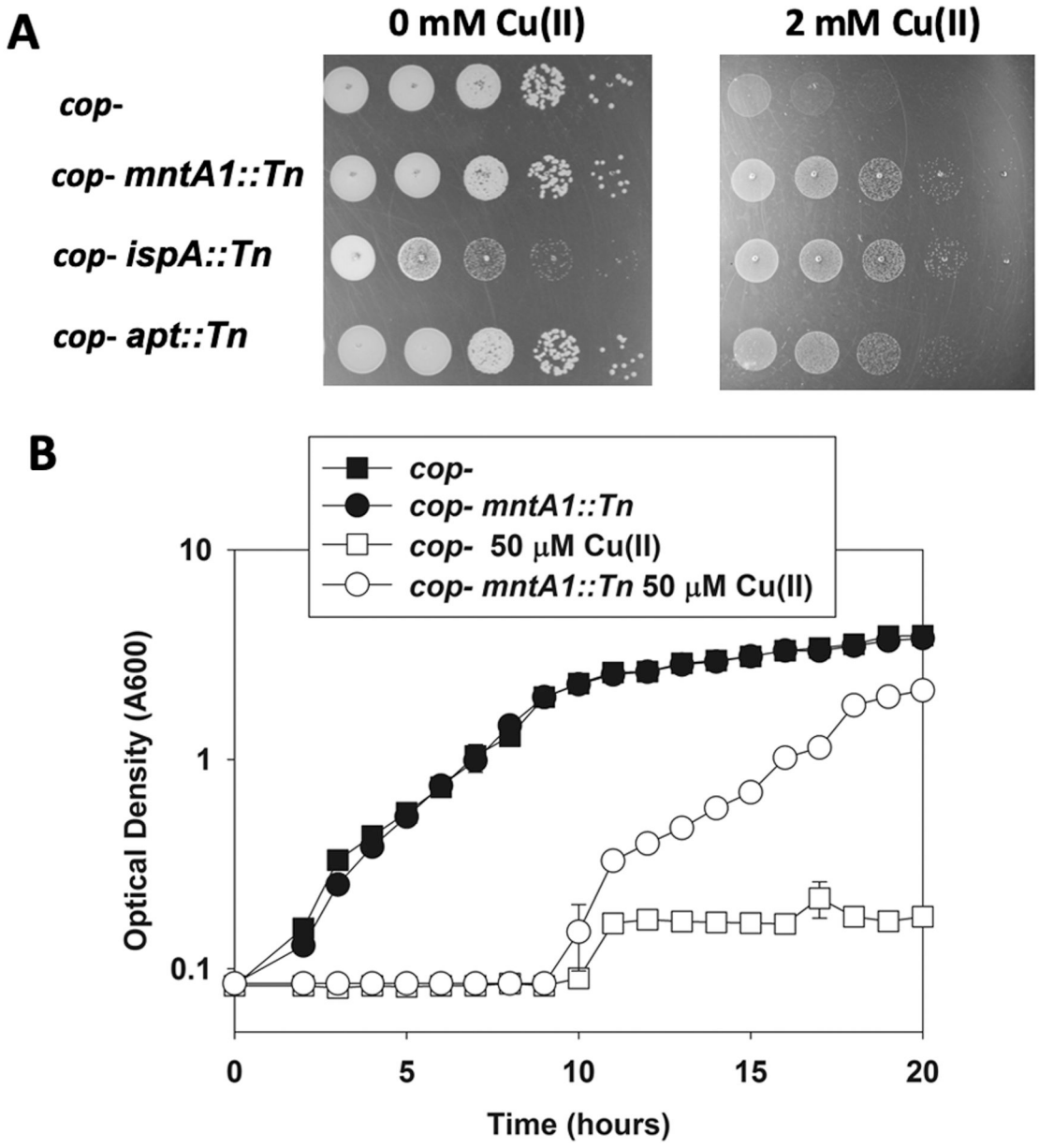

Figure 2. *S. aureus* strains with individual transposon insertions have increased growth in the presence of Cu.

Panel A; Overnight cultures of the *cop-* (JMB8573), *cop- mntA1::Tn* (JMB8914), *cop- apt::Tn* (JMB 8902), and *cop- ispA::Tn* (JMB8898) strains were serial diluted and spot plated on TSB medium containing 0 (no addition) or 2 mM Cu(II). Photos from a representative experiment are shown. Panel B; Overnight cultures of the *cop-* (JMB8573) and *cop- mntA1::Tn* (JMB8914) were diluted to 0.05 OD (A600) in liquid TSB medium with and without 50 μM Cu and culture density was monitored over time. The data represent the mean of three biological replicates and errors are presented as standard deviations. Error bars are included for all data, but often obscured by the symbol.

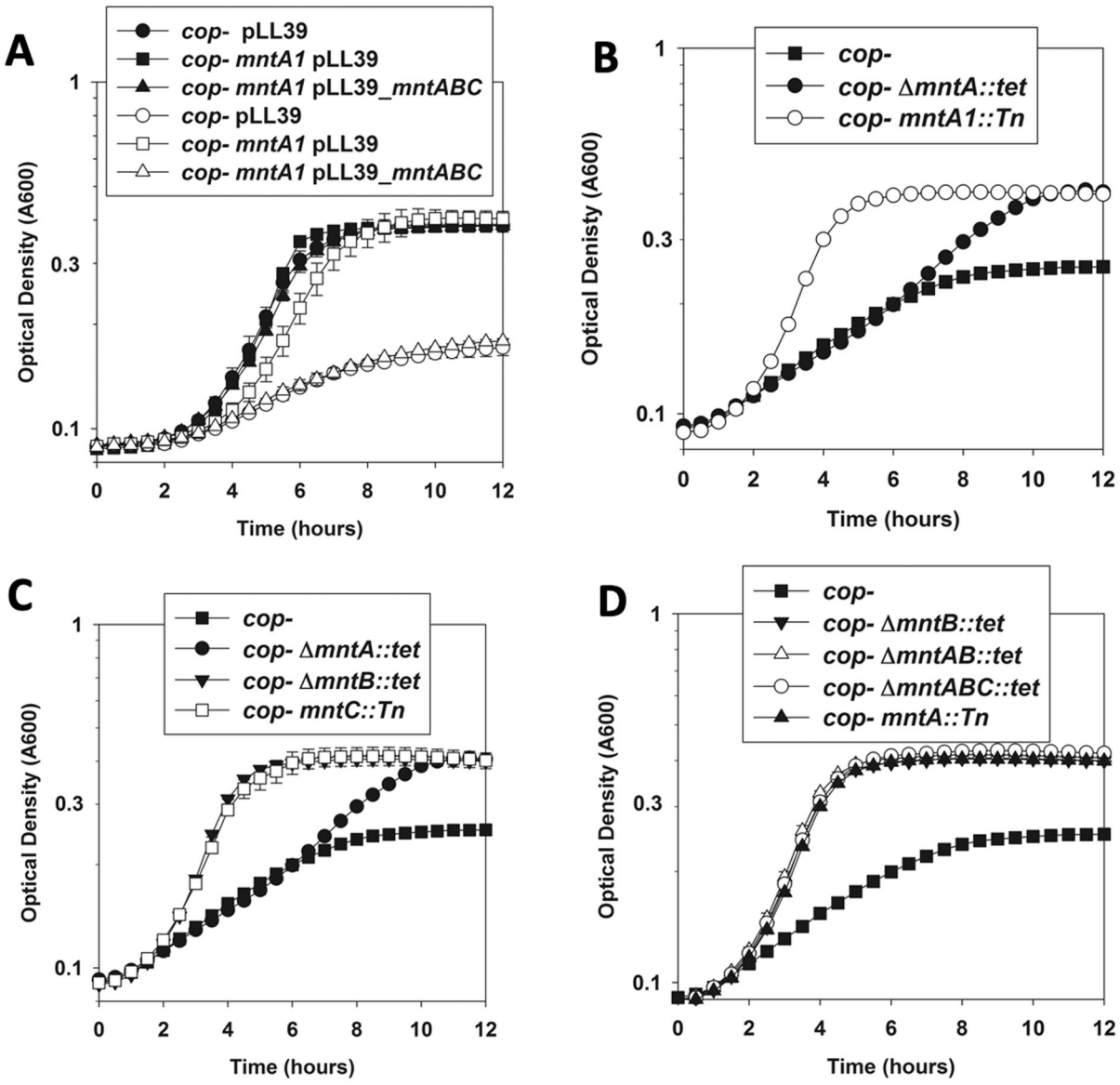

Figure 3. The *mntA1::Tn* mutation is recessive and null mutants in *mntA*, *mntB*, or *mntC* promote growth in the presence of Cu(II).

Growth was monitored in chemically defined media containing 20 amino acids (AA) with and without copper. Panel A; Genetic complementation of the Cu(II) resistance phenotype of the *cop- mntA1::Tn* strain. Growth of the *cop-* pLL39 (circles; JMB9535), *cop- mntA1::Tn* pLL39 (squares; JMB9534), and *cop- mntA1::Tn* pLL39_*mntABC* (triangles; JMB9469) in the presence (non-filled symbols) and absence (filled symbols) of 15 μM Cu(II) is shown. Panel B; A Δ*mntA::tetR* allele partially protected against Cu(II) intoxication. Growth of the *cop-* (squares; JMB8573), Δ*mntA::tetR* (black circles; JMB 9201), and *mntA1::Tn* insertion (white circles; JMB8914) in the presence of 20 M μCu(II) is shown. Panel C; non-functional *mntA::tetR*, *mntB::tetR*, and *mntC::Tn* alleles improve the growth of the *cop-* strain in the presence of Cu(II). Growth of the *cop-* (filled squares; JMB8573), *cop-* Δ*mntA::tetR* (circles; JMB 9201), *cop-* Δ*mntB::tetR* (triangles; JMB9208), and *cop- mntC::Tn* (white

squares; JMB 8965) in the presence of 20 M μCu(II) is shown. Panel D; the phenotypes associated with null mutants in *mntA*, *mntB*, and *mntC* are not genetically additive. Growth of the *cop-* (squares; JMB8573), Δ*mntA::tetR* (filled circles; JMB 9201), and Δ*mntB::tetR* (filled triangles; JMB9208), Δ*mntAB::tetR* (open triangles; JMB9246), Δ*mntABC::tetR* (open circles; JMB9325) in the presence of 20 μM Cu(II) is shown. The data represent the mean of two biological replicates and errors are presented as standard deviations. Error bars are included for all data, but often obscured by the symbol.

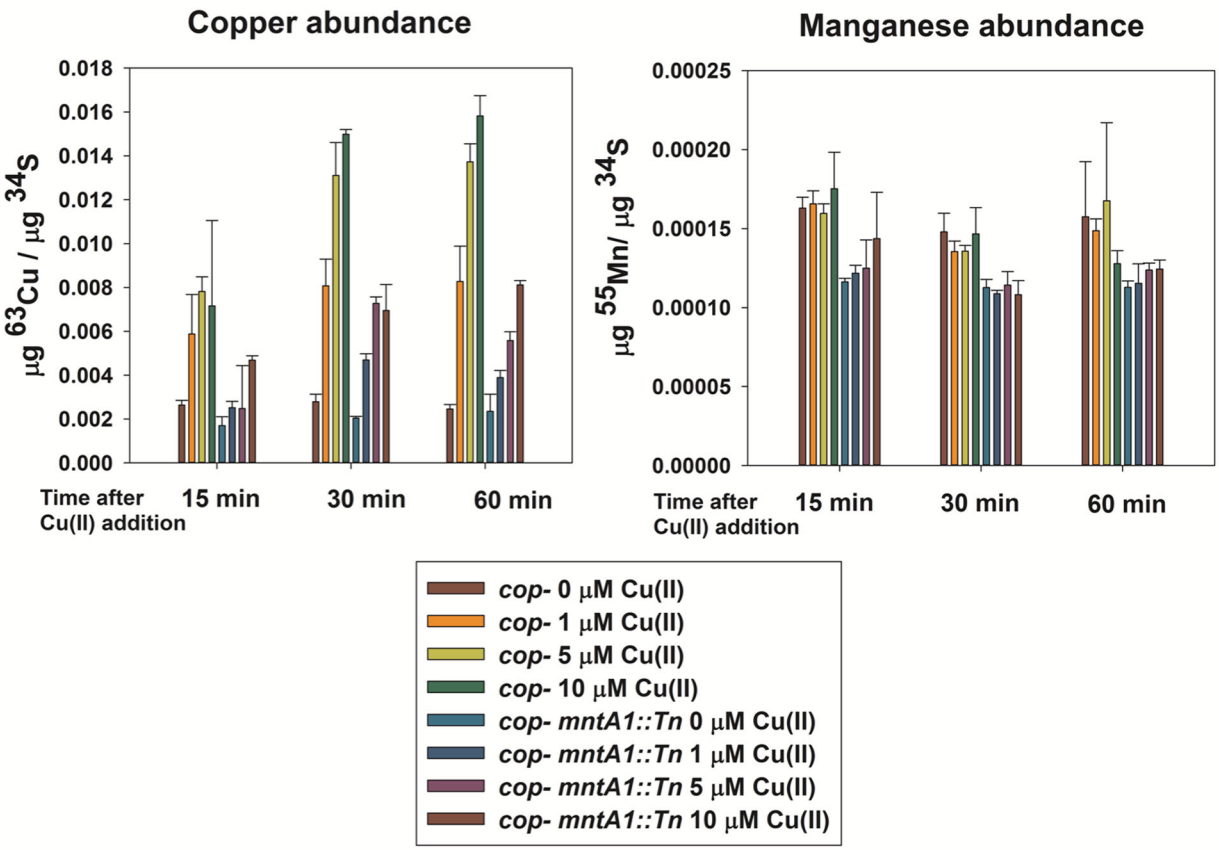

Figure 4. The *cop- mntA1::Tn* strain accumulate less Cu post challenge.

Cultures of the *cop-* (JMB8573) and *cop- mntA1::Tn* (JMB8914) strains were cultured in chelex treated TSB and challenged with 1,5, and 10 μM Cu(II) and incubated for an additional 15, 30, or 60 minutes before harvesting and determining Cu load by ICP-MS. Data showing total cellular Cu and total cellular Mn are shown. The data represent the mean of three biological replicates and errors are presented as standard deviations.

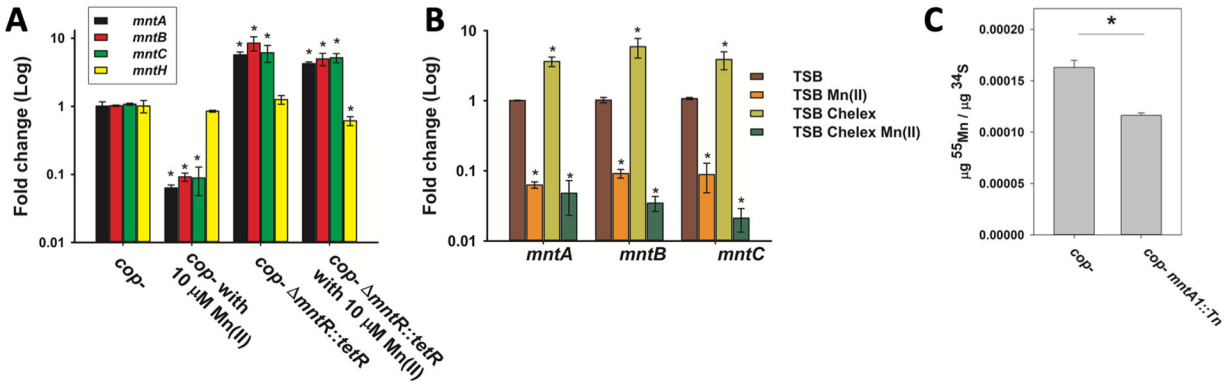

Figure 5. MntR represses transcription of the *mntABC* in a manganese-dependent manner under the growth conditions utilized.

Panel A; The data show fold-induction of *mntA*, *mntB*, *mntC*, and *mntH* in the *cop-* (JMB8573) and *cop-* Δ*mntR::tetR* (JMB9151) strains. The strains were cultured in TSB with and without 10 μM Mn(II) before RNA was isolated and transcripts quantified. Panel B; Data represent fold-induction of *mntA*, *mntB*, and *mntC* in the *cop-* (JMB8573) strain after culture in TSB, TSB with 10 μM Mn(II), Chelex treated TSB, or Chelex treated TSB with 10 μM Mn(II). Panel C; Total ^{55}Mn was quantified in the *cop-* (JMB8573) and *cop- mntA1::Tn* (JMB8914) strains using ICP-MS after the strains were cultured for 8 hours in Chelex-treated TSB. The data presented in Panels A, B, and C represent the average of biological triplicates with errors presented as standard deviations. Paired student t-tests were performed on the samples and N.S. denotes not significant ($p > 0.\ 0.05$) and * denotes $p \leq 0.05$.

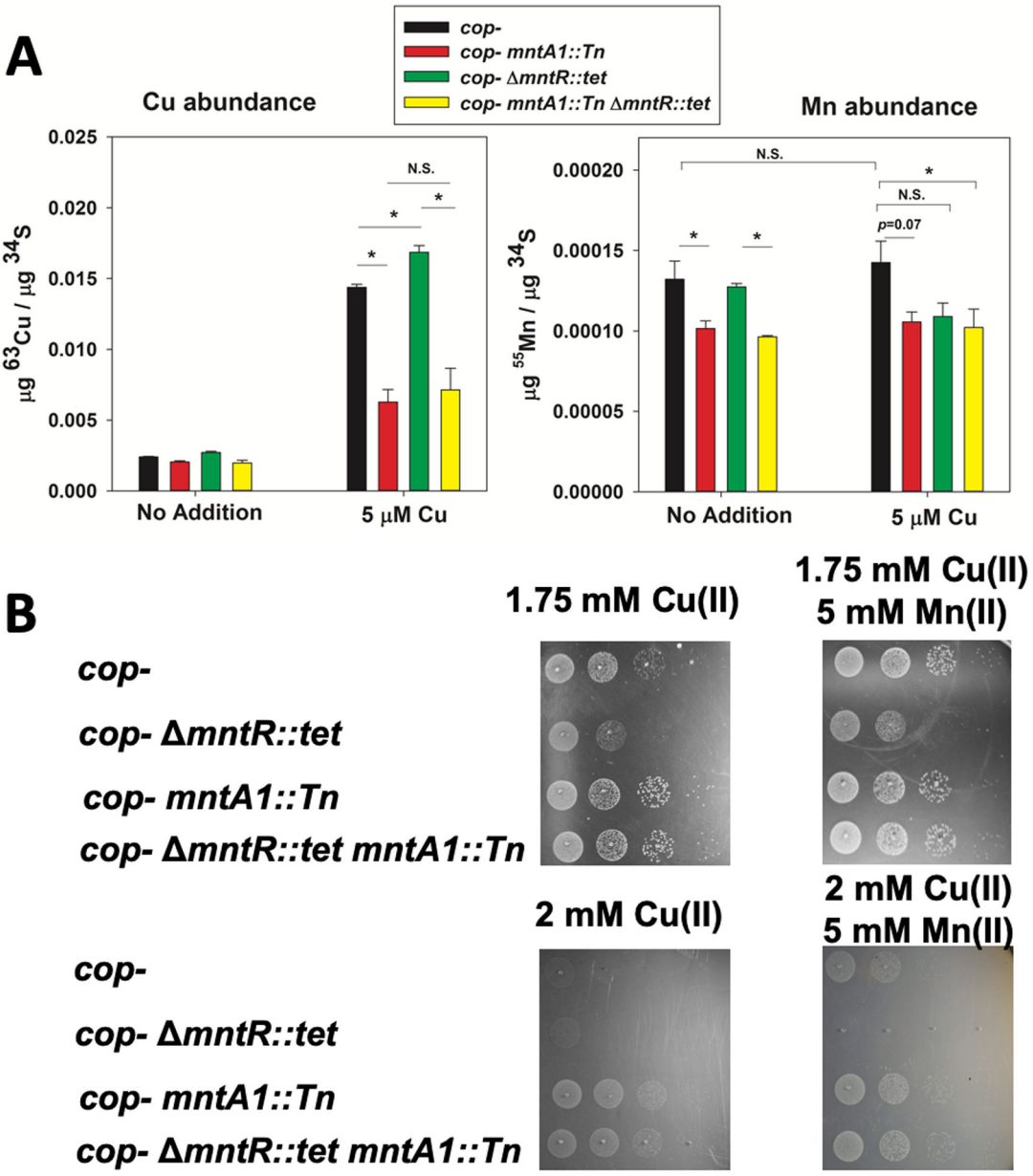

Figure 6. Derepression of the *mntABC* operon results in an increased Cu load and Cu sensitivity.

Panel A; the *cop-* (JMB8573), *cop- mntA1::Tn* (JMB8914), *cop-* Δ*mntR::tet* (JMB9151), and *cop-* Δ*mntR::tet mntA1::Tn* (JMB9244) strains were cultured in Chelex-treated TSB for 8 hours before challenge with 5 μM Cu for 60 minutes before quantifying total Cu and Mn loads using ICP-MS. Panel B; *cop-* (JMB8573), *cop- mntA1::Tn* (JMB8914), *cop-* Δ*mntR::tet* (JMB9151), and *cop-* Δ*mntR::tet mntA1::Tn* (JMB9244) strains were spot plated on solid TSB medium with 1.75 or 2 mM Cu and 0 or 5 μM Mn. The data in Panel A represent the mean of three biological replicates and errors are presented as standard deviations. Paired student t-tests were performed on the samples and N.S. denotes not significant ($p > 0.05$) and * denotes $p \leq 0.05$. Photos from a representative experiment are shown in Panel B.

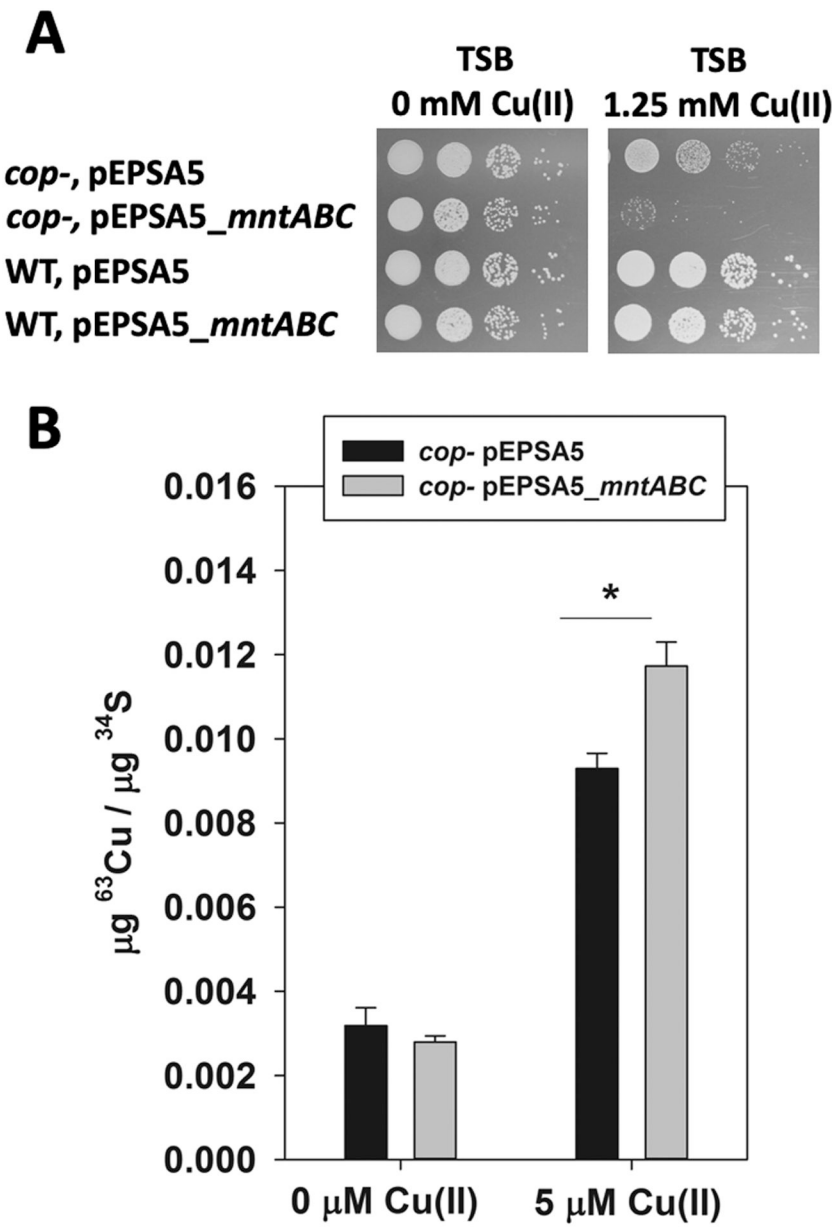

Figure 7. Over-production of MntABC increases sensitivity to Cu and increases the cellular Cu load.

Panel A; the *cop-* pEPSA5 (JMB9062) , *cop-* pEPSA5_*mntABC* (JMB9397) , WT pEPSA5 (JMB1304) , and WT pEPSA5_*mntABC* (JMB9478) overnight cultures were serial diluted and spot platted on TSB solid media containing 0.08 % xylose with and without 1.25 mM Cu(II). Panel B; the *cop-* pEPSA5 (JMB9062) and *cop-* pEPSA5_*mntABC* (JMB9397) strains were grown in Chelex-treated TSB for 8 hours before challenge with 5 µM Cu(II) for 15 min. Cells were harvested and Cu quantified using ICP-MS. The data represent the mean of three biological replicates and errors are presented as standard deviations. Paired student t-tests were performed on the samples and N.S. denotes not significant ($p > 0.1$) and * denotes $p \leq 0.05$. Photos from a representative experiment are shown in Panel A.

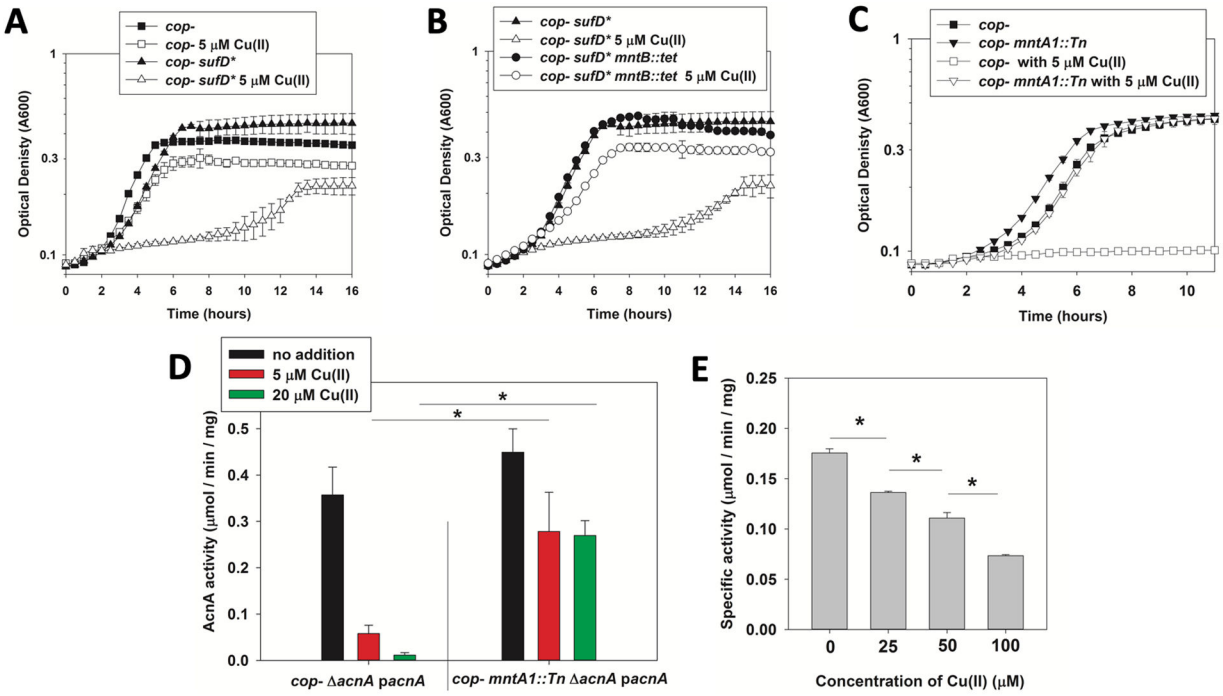

Figure 8. Defective MntABC protects iron-sulfur proteins from Cu poisoning.

Panel A; Growth of the *cop-* (JMB8573) and *cop- sufD** (JMB8625) strains were monitored in defined medium in the presence and absence of 5 μM Cu(II). Panel B; Growth of the *cop- sufD** (JMB8625) *cop- sufD** Δ*mntB::tetR* (JMB9604) strains was monitored in defined medium in the presence and absence of 5 μM Cu(II). Growth in panels A and B was monitored in chemically defined media containing 20 amino acids (AA). Panel C; Growth of the *cop-* (JMB8573) and *cop- mntA1::Tn* (JMB8914) strains in defined medium containing 18 amino acid medium lacking leucine and isoleucine with and without 5 μM Cu(II). Panel D; AcnA activity was monitored in cell-free lysates from the *cop- acnA::tetR* and *cop- acnA::tetR mntA1::Tn* strains containing pEPSA5_*mntABC* after culture in presence of 0–20 μM Cu(II). Panel E. AcnA activity was monitored in cell-lysates generated from the *cop-* strain cultured without Cu. The lysates were treated with Cu before assaying AcnA. The data in panels A-C represent the average of biological duplicates with error expressed as standard deviations. The data in panels D and E represent the average of triplicates or biological triplicates (panel D) with error expressed as standard deviations. Paired student t-tests were performed on the samples in D and E and N.S. denotes not significant ($p > 0.05$) and * denotes $p \leq 0.05$.

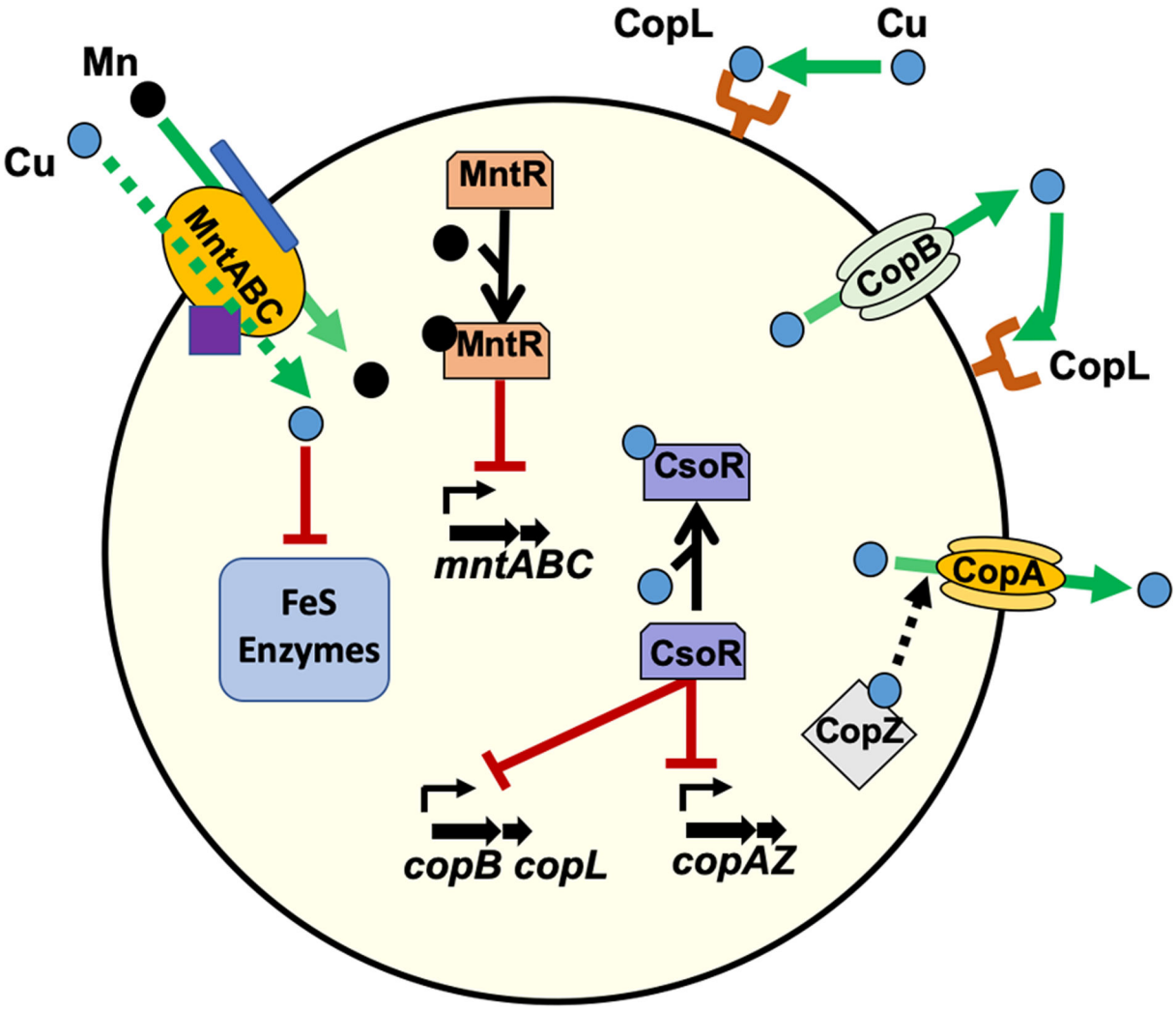

Figure 9. Working model for copper ion homeostasis in *Staphylococcus aureus*.

Under Mn deplete conditions, MntR derepresses *mntABC* transcription and *mntABC* is expressed. Cu enters *S. aureus* cells in a MntABC-dependent manner. Once the Cu ions have entered the cell, they are sensed by the CsoR transcriptional regulator. Cu association with CsoR results in derepression of the *copAZ* and *copBL* operons. CopA and CopB function as Cu(I) export systems. CopZ acts as an intracellular Cu(I) binding protein that buffers the cytosol from Cu toxicity. Holo-CopZ traffics Cu(I) to CopA for export. After export by CopA or CopB, or before Cu enters the cell, CopL binds to Cu(I) and prevents it from (re)entering.

Table 1.

Microbial strains and plasmids used in this study.

Microbial strains utilized in this study		
Name	**Chromosomal Genotype**	**Allele or strain reference**
***S. aureus* USA300 LAC strains**		
JMB 1100	USA300 wild-type strain- LAC	AR Horswill
JMB 1432	*fur::tetR*	(Horsburgh *et al.*, 2001, Mashruwala & Boyd, 2017)
JMB 8571	Δ*copAZ* (SAUSA300_2494–5)	This study
JMB 7901	Δ*copBL* (SAUSA300_0078–9)	(Rosario-Cruz *et al.*, 2019)
JMB 9621	Δ*copBL mntA1::Tn* (*ermB*) (SAUSA300_0620)	This study and (103)
JMB 8573	Δ*copBL* Δ*copAZ* (*cop*-)	This study
JMB 8914	*cop- mntA1::Tn* (*ermB*) (SAUSA300_0620)	This study
JMB 8915	*cop- mntA2::Tn* (*ermB*) (SAUSA300_0620)	This study
JMB 8898	*cop- ispA::Tn* (*ermB*) (SAUSA300_1470)	This study
JMB 8902	*cop- apt::Tn* (*ermB*) (SAUSA300_1591)	This study
JMB 9313	*mntA1*:: *Tn* (*ermB*) (SAUSA300_0620)	This study
JMB 8965	*cop- mntC::Tn* (ermB) (SAUSA300_0618)	This study
JMB 9977	*cop-* Δ*rsaC::tetR*	This study
JMB 10082	*cop- mntA1::Tn* (*ermB*) Δ*rsaC::tetR*	This study
JMB 9201	*cop-* Δ*mntA::tetR*	This study
JMB 9208	*cop-* Δ*mntB::tetR* (SAUSA300_0619)	This study
JMB 9325	*cop-* Δ*mntABC::tetR* (SAUSA300_0619–21)	This study
JMB 9151	*cop-* Δ*mntR:tetR* (SAUSA300_0621)	This study
JMB 9244	*cop-* Δ*mntR:tetR mntA1::Tn* (*ermB*)	This study
JMB 8625	*cop- sufD**	This study and (Roberts *et al.*, 2017)
JMB 9604	*cop- sufD** Δ*mntB::tetR*	This study and (Roberts *et al.*, 2017)
JMB 9535	*cop- attP::pLL39*	This study
JMB 9534	*cop- mntA1::Tn* (*ermB*) *attP::pLL39*	This study
JMB 9469	*cop- mntA1::Tn* (*ermB*) *attP::pLL39_mntABC*	This study
JMB 9320	*cop- acnA::tetR*	This study and (Somerville *et al.*, 2002)
JMB 9517	*cop- mntA1::Tn* (*ermB*) *acnA::tetR*	This study and (Somerville *et al.*, 2002)
JMB 8723	*cop- csoR::Tn*	This study and (Fey *et al.*, 2013)
Other microbial strains		
S. aureus RN4220	Restriction minus for transformation	(Kreiswirth *et al.*, 1983)
Escherichia coli PX5α	Used for molecular cloning	Protein Express
Saccharomyces cerevisiae FY2	Used for YCC cloning	13
Plasmids used in this study		
Name	**Function**	**reference**
pJB38	Construction of gene deletions	(Bose *et al.*, 2013)
pJB38_*rsaC::tetR*	Construction of *rsaC* deletion	This study
pJB38_Δ*mntA::tetR*	Construction of *mntA* deletion	This study
pJB38_Δ*mntB::tetR*	Construction of *mntB* deletion	This study

pJB38_Δ*mntABC::tetR*	Construction of *mntABC* deletion	This study
pJB38_Δ*mntR::tetR*	Construction of gene deletion	This study
pEPSA5	XylR dependent transcription	(Forsyth *et al.*, 2002)
pEPSA5_*mntABC*	*mntABC* under xylose inducible promoter	This study
pEPSA5_*acnA_FLAG*	AcnA expression	(Mashruwala *et al.*)
pLL39	Genetic complementation	(Luong & Lee, 2007)
pLL39_*mntABC*	*mntA::Tn* complement	This study
pMG020	Tn library generation	(Grosser *et al.*, 2018)
pBursa	Tn library generation	(Bae *et al.*, 2008)
pLL2787	Use to generate *attP::pLL39* integrant	(Luong & Lee, 2007)
pML100	TetR dependent transcription	(Lei *et al.*, 2011)
pML100_*rsaC*	Expresses *rsaC*	This study
pML100_*rsaC*-antisense	Expresses antisense *rsaC*	This study

Abbreviations: Tn, transposon

Table 2.

Primers used in this study

Primer name	Sequence
Ycc Pjb38 forward	AATAGGCGTATCACGAGGCCCTTTCGTCTTCAAGAATTCGGTGGCACT TTTCGGGGAAA
Ycc rseA rev	ACCTGATGAATAGCCACCTGAACGGCTAGCGCACATTAGGACCGTTATAGTTACGCTAT
Ycc rseA for	ATAGCGTAACTATAACGGTCCTAATGTGCGCTAGCCGTTCAGGTGGCTATTCATCAGGT
rseA tetR for	TATTAAAAGGTTGAAATGGTAGAGATAGCACGCGTCGGATTTTATGACCGATGATGAAG
rseA tetR rev	CTTCATCATCGGTCATAAAATCCGACGCGTGCTATCTCTACCATTTCAACCTTTTAATA
tetR rseA for	TATAAACATTCTCAAAGGGATTTCTAAACGCGTAGATCGATGTGTAACATTACGTTCTA
tetR rseA rev	TAGAACGTAATGTTACACATCGATCTACGCGTTTAGAAATCCCTTTGAGAATGTTTATA
rseA pJB38 rev	CTAGAGGATCCCCGGGTACCGAGCTCGAATTCCGAAATGCCAAGCTCAAAGTACATCCA
YCC CopAZ rev	GGACCT AATTGT GGA TTC TAC ACG CTA GCG CAC ATT AGG ACC GTT ATA GTT ACG CTA T
CopAZ Up for	ATA GCG TAA CTA TAA CGG TCC TAA TGT GCG CTA GCG TGT AGA ATC CAC AAT TAG GTC C
CopAZ up rev	CGA CAT CGT AAC CTT GAT CTT CAC GCG TGT CAT ACC AGT GAT ATC TAA TGT TG
CopAZ dwn for	CAACATTAGATATCACTGGTATGACACGCGTGAAGATCAAGGTTACGATGTCG
pJB38 CopAZ rev	CTA GAG GAT CCC CGG GTA CCG AGC TCG AAT TCG ACA ATG TTG AAG GTG TCG CTG G
YccmntRfor	AGC GTA ACT ATA ACG GTC CTA ATG TGC GCT AGC AAG ATT CTA ATT CTA AAT CGC TTA AT
mntRtetRrev	TTT CTT CAT CATCGG TCA TAA AAT CCG ACG CGT ACT TTC ACC TCA CAT ACA TTG TCT AT
tetRmntRfor	GTA TAT AAA CAT TCT CAA AGG GAT TTC TAA AAT AAA GAA GCC ATA AAG ATA TCC ATG AT
pJB38mntRrev	TAG AGG ATC CCC GGG TAC CGA GCT CGA ATT CTA TTA TGT TAT TGA TAG GTT TAG CGT CG
mntRtetRfor	ATA GAC AAT GTA TGT GAG GTG AAA GTA CGC GTC GGA TTT TAT GAC CGA TGA TGAAGA AA
tetRmntRrev	ATC ATG GAT ATC TTT ATG GCT TCT TTA TTT TAG AAA TCC CTT TGA GAA TGT TTA TAT AC
YCCmntAfor	ATA GCG TAA CTA TAA CGG TCC TAA TGT GCG CTA GCC CAG CGT CCG AGT CCA CAG TGG GA
mntAtetRfor	CTT TTA ATT AGG AGGTAT AAA CGA CGC GTC GGA TTT TAT GAC CGA TGA TGAAGA AAA GA
mntAtetRrev	TCT TTT CTT CAT CATCGG TCA TAA AAT CCG ACG CGT CGTTTA TAC CTC CTA ATT AAA AG
tetRmntAfor	ATA TAA ACA TTC TCA AAG GGA TTT CTA ACC ACCATG ATC TAT CAA AAG CAA AGC AAT AC
tetRmntArev	GTA TTG CTT TGC TTT TGA TAG ATC ATG GTG GTT AGA AAT CCC TTT GAG AAT GTT TAT AT
pJB38mntArev	ACT CTA GAG GAT CCC CGG GTA CCG AGC TCG AAT TCT GTG GCC TAA AAT ATT GGA GAT AC
tetRmntABrev	GGT ACT AAT TTT TTC ATG TTA AAC TTC CTC GTT AGA AAT CCC TTT GAG AAT GTT TAT AT
tetRmntABfor	ATA TAA ACA TTC TCA AAG GGA TTT CTA ACG AGG AAG TTT AAC ATG AAA AAATTA GTA CC
YCCmntABCfor	ATA GCG TAA CTA TAA CGG TCC TAA TGT GCG CTA GCC GTT ATT GTT GCA GCT TGT TAT AT
mntABCtetRrev	TCT TTT CTT CAT CATCGG TCA TAA AAT CCG ACG CGT TTC TAA CAA ACG TTT ATA CCT CC
mntABCtetRfor	GGA GGT ATA AAC GTT TGT TAG AAA CGC GTC GGA TTT TAT GAC CGA TGATGA AGA AAA GA
tetRmntABCrev	TCT TAC TTC ATT AAA ACA CAG CGT GTT ATT AGA AAT CCC TTT GAG AAT GTT TAT ATA
tetRmntABCfor	TAT ATA AAC ATT CTC AAA GGG ATT TCT AAT AAC ACG CTG TGT TTT AAT GAA GTA AGA
pJB38mntABCrev	ACT CTA GAG GAT CCC CGG GTA CCG AGC TCG AAT TCA GTA GGG AGA ACA GTT GTC CAA TC
pJB38mntABCrev	ACT CTA GAG GAT CCC CGG GTA CCG AGC TCG AAT TCA GAT GAA GTA TCA GAA GGT ACA GC
pEPmntABCfor	CCTCTAGAGTCGACTTAGGAGGATGATTATTT TTGTTAGAAACAAAAGATTTAAATCTG
mntABCYCCrev	GCG TAA CTT TTC CCC GAA AAG TGC CAC CACGCG TGG TAA TAT ATA TTT AAC GCA CGA TA
pLLYCC5	CTG TAA TGG GCC CAA TCA CTA GTG AAT TCC CGA AGC GGT GGC ACT TTT CGG GGA AA
mntABCYCC3	AAA GAG GAC TAT TTA AAG GCA ATC CTT ACG CTA TAT TAC CCT GTT ATC CCT A
YccmntABC	TAG GGA TAA CAG GGT AAT ATA GCG TAA GGA TTG CCT TTA AAT AGT CCT CTT T

Primer name	Sequence
mntABCpLL39	GTG CTA AAG AAGTTG TAG GTA ATA AAA AAG CTT GCC AAT ATT TTA GGT TGC ATC AAC ATC
upRsaCtetfwd	CGAAGGCTAATAGTCCCATATCGTGCGCGGATTTTATGACCGATGATGAAGAAAAG
tetupRsaCrev	CTTTTCTTCATCATCGGTCATAAAATCCGCGCACGATATGGGACTATTAGCCTTCG
downRsaCtetrev	ATAGCCACACTCATATGACATCGGTTAGAAATCCCTTTGAGAATGTTTATATACATTCAAGG
tetdownRsaCfwd	CCTTGAATGTATATAAACATTCTCAAAGGGATTTCTAACCGATGTCATATGAGTGTGGCTAT
pJB38rsaCrev	ACTCTAGAGGATCCCCGGGTACCGAGCTCGAATTCGCCATTATTAACGAAACCTGCACCTAAAACAG
YCCrsaCfor	ATAGCGTAACTATAACGGTCCTAATGTGCGCTAGCGACGAATTCAATTTTATATGATATGGCTAAAAATG
RsaCSalIantisense	GGGGTCGACGGTGAAGTTAAGTGTATTCACAAAAAATAGCCACACTCATATG
RsaCEcoRIantisense	GGGGAATTCGGCCACACATCAACATAACAAAGTCGAAGGCTAATAGTCCCATATC
RsaCSalIsense	GGGGTCGACGGCCACACATCAACATAACAAAGTCGAAGGC
RsaCEcoRIsense	GGGGAATTCGGTGAAGTTAAGTGTATTCACAAAAAATAGCCACACTCATATG
Rt_mntC Fwd	GCA GTG ATA AGT CAA ATG GCA AAT T
Rt_mntC rev	TCT CCA CCAACA TTT TTA GCC ATA
Rt_mntA fwd	ATA CCA GTA CGC GGC GAA ATA
Rt_mntA rev	AGG GAA GAT TTA CCA GCA CCA TT
Rt_mntB fwd	TCA CGC AGT ATT ACC TGG TGT TG
Rt_mntB rev	ACC AGT TAT AAG TGC GCC TAC AAA
Rt_mntH fwd	TTA GTC GCT GTT GGT TAC ATG GA
Rt_mntH rev	GCG CCA CCT TGC ATT GAT
16sfwdRT	TGA AAG CCC ACG GCT CAA
16srevRT	TTC TGC ACT CAA GTT TTC CAG TTT
gyrAfor	GGACGTCAACGTATTGTTGTCACT
gyrARev	CGAGCTCTGCAATTTTTTCAATC
SCV8	GCACATAATTGCTCACAGCCA
SCV9	GCTGATCTAACAATCCAATCCA
Tn Buster	GCTTTTTCTAAATGTTTTTTAAGTAAATCAAGTACC
Martn-ermR	AAACTGATTTTTAGTAAACAGTTGACGATATTC